US ARMY
LABORATORY COMMAND
MATERIALS TECHNOLOGY
LABORATORY

MTL TR 85-37

DETECTION AND LOCATION OF BALLISTIC DAMAGE IN COMPOSITE MATERIALS USING ACOUSTIC EMISSION METHODS

December 1985

J. F. JAMINET, M. W. HAWMAN, and R. S. WILLIAMS
United Technologies Research Center
East Hartford, CT 06108

Final Report

Contract No. DAAG46-84-C-0054

Prepared for

U.S. ARMY MATERIALS TECHNOLOGY LABORATORY
Watertown, Massachusetts 02172-0001

The findings in this report are not to be construed as an official Department of the Army position, unless so designated by other authorized documents.

Mention of any trade names or manufacturers in this report shall not be construed as advertising nor as an official indorsement or approval of such products or companies by the United States Government.

DISPOSITION INSTRUCTIONS

Destroy this report when it is no longer needed.
Do not return it to the originator.

UNCLASSIFIED

SECURITY CLASSIFICATION OF THIS PAGE (When Data Entered)

REPORT DOCUMENTATION PAGE		READ INSTRUCTIONS BEFORE COMPLETING FORM
1. REPORT NUMBER MTL TR 85-37	2. GOVT ACCESSION NO.	3. RECIPIENT'S CATALOG NUMBER
4. TITLE (and Subtitle) DETECTION AND LOCATION OF BALLISTIC DAMAGE IN COMPOSITE MATERIALS USING ACOUSTIC EMISSION METHODS		5. TYPE OF REPORT & PERIOD COVERED Final Report - Sep 84 to Oct 85 6. PERFORMING ORG. REPORT NUMBER
7. AUTHOR(s) J. F. Jaminet, M. W. Hawman, and R. S. Williams		8. CONTRACT OR GRANT NUMBER(s) DAAG46-84-C-0054
9. PERFORMING ORGANIZATION NAME AND ADDRESS United Technologies Research Center East Hartford, CT 06108		10. PROGRAM ELEMENT, PROJECT, TASK AREA & WORK UNIT NUMBERS D/A Project: 1L162105AH84 AMCMS Code: 612105.H84
11. CONTROLLING OFFICE NAME AND ADDRESS U.S. Army Materials Technology Laboratory ATTN: SLCMT-ISC Watertown, Massachusetts 02172-0001		12. REPORT DATE December 1985 13. NUMBER OF PAGES 62
14. MONITORING AGENCY NAME & ADDRESS (if different from Controlling Office)		15. SECURITY CLASS. (of this report) Unclassified 15a. DECLASSIFICATION/DOWNGRADING SCHEDULE

16. DISTRIBUTION STATEMENT (of this Report)

Approved for public release; distribution unlimited.

17. DISTRIBUTION STATEMENT (of the abstract entered in Block 20, if different from Report)

18. SUPPLEMENTARY NOTES

19. KEY WORDS (Continue on reverse side if necessary and identify by block number)

Acoustic emission	Composite materials
Ballistic impact	Helicopters
Impact damage	Survivability

20. ABSTRACT (Continue on reverse side if necessary and identify by block number)

(SEE REVERSE SIDE)

DD FORM 1 JAN 73 1473 EDITION OF 1 NOV 65 IS OBSOLETE

UNCLASSIFIED

SECURITY CLASSIFICATION OF THIS PAGE (When Data Entered)

Block No. 20

ABSTRACT

A method for increasing survivability is described whereby the acoustic emissions generated by ballistic impacts on composite helicopter structural components are recorded and analyzed using a preliminary digital transient data recording test system, the Digital Acoustic Emission System (DAES) and lightweight sensors utilizing polyvinylidene fluoride (PVDF) film. A total of 77 ballistic impacts on six composite test segments using a variety of fragment simulating projectiles (FSP) with different muzzle velocities and impact energies is described. The results verify the capability of the measurement system to detect, locate, and analyze the severity of ballistic impacts. The ratio of the peak RMS value of the output signal from two sensors is shown to be a good indicator of impact energy absorption, or damage severity. Calculated hit locations are found with a mean error of seven percent of the sensor array edge distance.

R85-997021-12

Detection and Location of Ballistic Damage in Composite Materials Using Acoustic Emission Methods

TABLE OF CONTENTS

LIST OF TABLES AND FIGURES

TABLES

FIGURES

1.0 PREFACE

The research reported herein was performed under Contract No. DAAG46-84-C-0054 for the Army Materials Technology Laboratory, Watertown, Massachusetts 02172. Mr. Robert Muldoon served as Technical Contract Monitor for the Army on this program. We are greatly indebted to the following people for their important contributions to this program: Mr. Malcolm Pierce (SA), who suggested the use of acoustic emission to monitor ballistic impacts; Mr. Raj Kaushik (SA) for his assistance in obtaining the composite test specimens; and Mr. Robert Haas (UTRC), for his assistance in conducting the ballistic testing.

2.0 PROGRAM SUMMARY

A program was conducted to demonstrate the feasibility of using quantitative acoustic emission methods to detect, locate, and classify in real-time ballistic impact damage in composite materials. The ultimate objective of this research is to provide an in-flight structural damage location and assessment system to enhance the survivability of a composite airframe helicopter. The prescribed immediate requirements of this program were to assemble, install, and ballistically test a prototype damage detection system using representative helicopter-type composite materials. All of these requirements were met successfully.

A prototype transient recording and analysis system for damage detection and location consisting of the UTRC Digital Acoustic Emission System (DAES), and related software were assembled for use in this program. A series of advanced, lightweight piezoelectric polyvinylidene fluoride (PVDF) film AE sensors, based upon a UTRC design, were fabricated for installation on composite helicopter components.

Six composite test structures representative of critical locations on a helicopter were instrumented with the PVDF sensors and ballistically tested using a variety of ammunition (5.6 mm to 7.62 mm) covering a wide range of muzzle velocities and impact energies. The tests were conducted at a commercial firing range in Wallingford, Connecticut. A total of 77 ballistic impacts were recorded, of which 26 were obtained using 7.62 mm (cal .30) fragment simulating projectile (FSP) ammunition. Acoustic emission waveforms resulting from these ballistic impacts were recorded and analyzed using the DAES. These analyses proved the feasibility of the concept and recommendations for flightworthy system implementations were developed.

The research reported herein was performed under Contract No. DAAG46-84-C-0054 for the Army Materials Technology Laboratory, Watertown, Massachusetts 02172.

3.0 RESULTS AND CONCLUSIONS

The results of the program verify the feasibility of developing a lightweight, airworthy battle damage assessment system utilizing acoustic emission methods. Specifically, the results show that:

1. Ballistic hits over a range of impact energies can be detected in composite structural components using the Digital Acoustic Emission System (DAES) with polyvinylidene fluoride (PVDF) film sensors. A total of 77 ballistic hits with impact energies ranging from 98 to 2780 ft-lbs were detected.

2. It is possible to assess the severity of damage caused by ballistic impacts on important structural areas (spars) versus non-structural areas (skins) by analysis of the AE waveforms. In particular, the ratio of the peak RMS signal values from two adjacent sensors appears to be a meaningful indication of damage severity since the effects of attenuation due to distance to the sensors are mitigated or eliminated. The average signal ratio of the on-spar to the off-spar hits was 12.9.

3. Hit locations can be calculated with reasonable accuracy using a four sensor array. The results indicate a mean error in hit location of approximately seven percent of the sensor array edge distances over a 20 in. square array.

4.0 RECOMMENDATIONS

Based on the results of the program, the following recommendations are made with the long-term goal of developing an operational, flightworthy system.

1. Development work should continue on the PVDF transducers to improve their sensitivity and reduce lot-to-lot variations in response. Furthermore, transducers should be developed to incorporate these sensors in the structure during manufacture.

2. A smaller "brass-board" dedicated data recording and analysis system should be designed and fabricated. This system would ultimately provide the basis for a miniaturized (VLSI) prototype flightworthy system.

3. Utilize the improved sensors and "brass-board" data acquisition and analysis system to obtain additional ballistic impact data from hits on a full size composite airframe such as the Sikorsky Aircraft ACAP tool-proof airframe. These measurements will provide a considerably increased database of ballistic impact information from a large helicopter structure typical of present and future aircraft. Data obtained from these tests would be used to program the prototype VLSI signal processing package.

5.0 INTRODUCTION

New rotary wing aircraft are being designed with a greater emphasis on the use of composite materials in both structural and non-structural components. In addition to the primary advantage of lighter weight for equivalent strength versus metallic structures, composite materials have proven to be ballistically tolerant. However, since the structure and potential failure modes of these materials are more complex than conventional materials, it is highly desirable to have a means of detecting, locating, and assessing the severity of battle damage. A review of data on helicopter losses in Vietnam (see Ref. 1) indicates that as many as 65% of battle losses were the result of 7.62 mm and 12.7 mm rounds. Present and future aircraft will be exposed to newer and more destructive threats (23 mm, 30 mm, 57 mm HEI) for which passive armor concepts are less effective. A high reliance will be placed on evasive tactics, including nap of the earth flying to combat these threats. However, it is anticipated that in these regimes, the lower energy ballistic 7.62 mm - 12.7 mm threats will continue to be significant causes of both attrition and forced landing kills. To insure the survivability of the helicopter and crew, an on-board battle damage assessment system is required to counter these threats. Such a system would determine the flight criticality of a ballistic hit and inform the pilot, permitting him to take appropriate action to save the aircraft. Developments in acoustics, signal processing, and micro-computers indicate that such a system is conceptually feasible.

The United Technologies Research Center (UTRC) and Sikorsky Aircraft (SA), under Internal Research and Development (IR&D) funding, initiated an investigation of acoustic emission (AE) detection of ballistic damage in mid-1982. These activities have continued to the present, culminating in the present contract to determine the feasibility of the approach on full-scale helicopter components subjected to realistic ballistic threats.

The earliest work in which the feasibility of acoustic emission monitoring of small arms ballistic damage was demonstrated for simple composite structures, was accomplished from May-September 1982 at UTRC with (IR&D) funding from SA. In this program, 30 cm x 30 cm Kevlar and graphite composite panels, fabricated by SA, were monitored for acoustic emission during ballistic impact. The results showed AE was capable of detecting and characterizing a ballistic hit. The sensors used consisted of two types, a point contact ceramic transducer (PCT) and an experimental transducer design utilizing polyvinylidene fluoride (PVDF) film.

In 1983, the UTRC/SA technical efforts were focused on transducer refinements and small arms ballistic damage of simple metallic structures with the ultimate goal of developing a system concept for a battle damage monitor for the Blackhawk helicopter, which incorporates both metallic and composite structures. Emphasis has since focused on composite structures as they represent a greater degree of difficulty in AE monitoring due to material anisotropy. A system developed for use with composites could also be used on metal structures such as those in the Blackhawk helicopter.

In 1983, the point contact transducer and the polyvinylidene fluoride sensor were refined for use in AE monitoring of battle damage. For the PCT, a new type of wear shoe was added that totally encapsulated the transducer and prevented electromagnetic interference (EMI). The PVDF sensor was vastly improved by decreasing the dimensions of the active element and by reducing the mass loading. The final 1983 version was small and lightweight, yet still retained adequate frequency response (greater than 2 MHz bandwidth).

Small arms ballistic tests were performed on a frame-stiffened aluminum panel in 1983. Ballistic damage was created by firing 5.6 mm 0.22 caliber (675 and 1150 ft/sec muzzle velocities) and 9.65 mm, 0.38 caliber (1000 ft/sec muzzle velocity) projectiles. The peak amplitudes of the acoustic signals were shown to correlate with the size of the projectiles, while the frequency content of the signal was shown to be an indicator of impact severity i.e., impact energy.

In January 1984, a study on small arms ballistic damage on the Advanced Composite Airframe Program (ACAP) helicopter structure was performed for Sikorsky Aircraft at the Army Applied Technology Laboratory (ATL), Fort Eustis, Virginia. Two different types of acoustic emission transducers, both developed at UTRC were used to monitor the impact of 12.7 mm armor-piercing (AP) shells on the ACAP helicopter structure. The objective of the study was to assess the feasibility of using either type of transducer to detect small arms damage in large helicopter type structures and to characterize the nature of the impact. The polyvinylidene fluoride (PVDF) film transducer proved to be more effective for ballistic monitoring than the point contact ceramic transducer (PCT). The PVDF transducer with its negligible mass loading was more sensitive to the high frequency content of the ballistic AE signal. Also, it maintained close coupling to the surface, thereby generating an output signal with both negative and positive amplitude time domain features. The PCT produced only positive amplitude signals because its inherently large mass caused it to break contact with the surface as the surface accelerated away from the transducer.

The difference in the AE response for different levels of ballistic damage was readily apparent. Two shots were fired at the main vertical spar; one hit the spar directly while the other merely grazed it. The shot that hit the spar directly generated an AE waveform with considerable high frequency content and amplitude, indicating a massive transfer of energy to the structure. In contrast, the other shot generated a waveform with much lower amplitude and frequency content. As in the previous laboratory studies at UTRC, these results were similar to those obtained for the small arms ballistic tests on the graphite/epoxy panels as well as the frame-stiffened aluminum panel. By monitoring a full scale helicopter structure during 12.7mm AP ballistic damage, it was shown that the laboratory test approach remained valid for large, complicated structures and that the PVDF transducer was preferred for ballistic impact monitoring.

During the remainder of 1984, the PVDF film transducer was further refined and improved. While retaining its minimum size and high frequency capability, fabrication methods were improved to increase its sensitivity and consistency from unit to unit. It was also during this time frame that the Digital Acoustic Emission System (DAES) for data acquisition, storage and analysis of AE waveforms was designed and assembled. The system incorporates a LeCroy 3500 transient recording and analysis system. Considerable software has been developed for this system to acquire, store, and analyze AE waveforms.

The present Contract was initiated in September 1984 to apply the PCT and PVDF transducers and the DAES to realistic ballistic damage scenarios. The following Sections describe the objective, technical approach, test results, and major conclusions and recommendations of the subject program.

6.0 PROGRAM OBJECTIVE

The objective of the research was to establish the feasibility of using quantitative acoustic emission methods to detect, locate, store, and assess the severity of damage due to ballistic impact on critical helicopter components. The primary goal is to improve the survivability of the aircraft and crew. A secondary goal is to improve the reliability and maintenance of the aircraft. The overall system concept for accomplishing this is outlined as follows.

6.1 Overall System Concept

In an operational, flightworthy system a helicopter would be instrumented with arrays of AE sensors located in critical structural areas as shown conceptually in Fig. 1. These sensors would be connected to a microprocessor-based signal processing package that would only communicate flight critical information to the pilot. Other information would be stored for analysis on the ground. The system would perform the following functions: (1) it would immediately detect, locate, and determine the severity of a ballistic hit on the helicopter; (2) it would monitor the progression of structural damage and warn the pilot of impending structural failure; (3) it would store the data (initial structural damage and progressive structural damage propagation) in memory for subsequent use and analysis by ground crews to determine the airworthiness of the helicopter.

6.2 Technical Approach

The focus of this program has been to define the feasibility and scope of a real-time, on-board, flightworthy ballistic damage warning system which would enhance the survivability of the helicopter and crew. From an aircraft and crew survivability standpoint, the primary goal is to detect ballistic hits on a component that could result in a mission abort and/or a forced landing in enemy territory. As shown in Fig. 1, the component areas of special interest are as follows:

1. Avionics Equipment Housing - A hit in this area could cause failure of flight or mission essential equipment. Early detection and pilot warning might prevent loss of the aircraft and crew.

2. Fuel Cells - A hit in this area could cause premature depletion of the usable fuel. The pilot could be warned in real-time to watch for a rapid reduction in fuel levels.

3. Transmission/Flight Control Area - A hit in the transmission or transmission support structure might cause rapid failure due to abnormalities such as gear fracture or fatigue, loss or contamination of oil, or catastrophic vibration. The pilot would be warned to closely monitor temperature or chip detector devices. A hit in the flight control/rotor servo cylinder area might cause an eventual loss of control of the aircraft which could be anticipated by the pilot if he were forewarned.

4. Engine Nacelle Area - A hit in the engine nacelle area might initiate a flame-out or engine fire due to combustor damage. Also, a hit in this area could cause damage to the engine mounts or input control shafts. In either case, an engine power reduction may be advisable or necessary.

5. Tail Rotor Driveshaft Housing and Gearbox - A hit in these areas could result in a flight control emergency due to a loss of the tail rotor function. The pilot might be forewarned to monitor temperature/chip detectors, be alert for unusual vibrations or to initiate a power reduction thus forestalling total failure of the tail rotor system.

6.3 Reliability and Maintainability Considerations

A secondary goal in implementing a system is to improve aircraft reliability and reduce maintenance time. Several important aspects are:

1. Damage/Failure Propagation - Continuous in-flight monitoring of known damage sites could be accomplished using a microprocessor based system. Assuming the development of a database relating AE activity with remaining component life, an appropriate warning could be given to the pilot not to continue flight or to the ground crew that the aircraft is no longer airworthy. By this method, maintenance of noncritical but potentially important items could be deferred until absolutely necessary. This could vastly improve ground turnaround time in combat situations and increase the number of sorties per aircraft significantly.

2. A repair/maintenance deferred/accomplished log in database form could be carried completely in microprocessor memory. Ground crews could interrogate the system to determine what new (or deferred) maintenance items were required to be performed prior to the next flight.

6.4 Technical Requirements

This program was divided into three tasks summarized as follows:

Task I - Assemble a prototype damage detection system capable of recording and digitizing acoustic emission data from ballistic impacts and crack initiations and propagation using advanced signal analysis techniques. Formulate pattern recognition algorithms to locate the damage zone and analyze the severity of damage. Design and assemble appropriate transducers including the point contact ceramic type. Demonstrate that the above system will function when the test specimens used in ballistic impact tests are fiber reinforced organic matrix composites.

Task II - Provide test specimens consisting of helicopter structural components such as tail booms, rotor blade sections, skins, and frame members with a total surface area equivalent to ten pieces with dimensions of 12 in. by 24 in. Ship the above components, as well as the test equipment assembled under Task I, to an appropriate firing range for ballistic impact testing. Instrument the test specimens with appropriate transducers and calibrate the data system at the firing range prior to testing.

Task III - Test prototype damage detection system by impacting the helicopter component test specimens with a minimum of ten and a maximum of fifty 7.62 mm (cal .30) fragment simulating projectiles (FSP). Analyze the resulting data to verify the capability of the damage detection system to detect, locate, and assess the severity of damage from these ballistic impacts.

7.0 TECHNICAL DISCUSSION

7.1 Task I - Prototype Damage Detection System

A prototype damage detection system capable of recording, digitizing, storing, and analyzing acoustic emission data from ballistic impacts and crack initiation/ propagation using advanced signal analysis techniques was assembled. This system is essentially the Digital Acoustic Emission System (DAES) developed by UTRC for use with the PCT and PVDF sensors, with line drivers added to accommodate extra long signal cables required for ballistic monitoring.

7.1.1 Digital Acoustic Emission System

The DAES is a combination of hardware, diagrammed in Fig. 2, and software which performs acquisition, storage, and analysis of AE data. The DAES hardware is configured around a LeCroy 3500 transient recording and analysis system. An eight channel Dunegan 8000 system was used for analysis of ballistic impact location.

The DAES system has the capability of digitizing four channels of AE signals at sampling rates up to 100 Mhz. Record lengths up to 295,000 data points can be stored with a future storage capability of 524,000 data points. These long record lengths are extremely important for applications involving continuous generation of acoustic emission such as crack propagation analysis.

The entire data acquisition, short term data storage, triggering and event timing hardware is modular. The capabilities of the system can be quickly modified for a specific application by the proper selection of hardware modules. Flexibility is inherent in the system computer controller. The set-up of the hardware, data acquisition, data storage and data analysis are all controlled through software. This software can take various forms including FORTRAN, C-Basic, assembly language, microcode and PROM based firmware. The computer also has several resident microprocessors including a bit-slice processor which can execute three instructions simultaneously, thereby providing the computational speed required for real-time signal processing.

Once the AE signal has been recorded, the data may be placed in long-term storage on floppy disk, hard disk, or 9-track magnetic tape. Post-test analysis can be performed through software installed on the DAES or the data can be downloaded to various mainframe computers for more extensive analysis.

7.1.2 Point Contact Transducer (PCT)

Quantitative analysis of acoustic emission cannot be successful without adequate sensors that can accurately detect AE events. Currently available commercial equipment does not meet the requirements for uniform broadband transducers. The point contact transducer was developed by UTRC to help resolve these limitations.

The PCT is a conical element, piezoelectric, broadband transducer with a frequency response, flat to within 5 dB, from a few kilohertz to approximately 1.5 MHz. The construction details of the PCT are shown in Fig. 3. The transducer consists of a small, conically-shaped PZT-5A (lead zirconate titanate) element bonded to the center of the highly polished face of a large brass cylinder. The tip of the conical PZT element which makes a contact with the test surface is ground flat. A passing surface wave causes the tip to be displaced and thereby generates a small voltage between the tip ground electrode and the brass cylinder backing which acts as the high signal side. The resulting voltage signal is subsequently processed.

The principle of operation of this transducer is straightforward. The small diameter tip has a point-like receiver response over the frequency range (1 kHz - 1 MHz) and thereby eliminates phase interference artifacts in the waveform response. The conical shape prevents buildup of specific standing waves in the tip which broadens the uniform bandwidth response in the higher frequency range. The brass cylinder serves several functions. The cylinder has a close acoustic impedance match to PZT-5A and will therefore couple out high frequency backward traveling waves in the conical element. These waves are then absorbed and lost in the brass thus avoiding interference with the incoming wave at the cone tip. However, this behavior is strongly dependent upon the bond integrity between the cone and brass. Consequently, a highly polished surface is required in order to provide a thin tight bond. Further, the brass adds a mass loading to the conical element thereby broadening its frequency response. The combined brass/cone element acts as a coupled resonator exchanging energy from the low frequencies, determined by the brass mass loading of the PZT element acting as a spring, to the high frequencies where the brass is essentially motionless (acting only as an absorber) and the PZT is vibrating against the brass.

7.1.3 Polyvinylidene Fluoride (PVDF) Transducer

Polyvinylidene fluoride (PVDF) belongs to a class of polymers known as ferroelectrics which exhibit piezoelectric and pyroelectric properties. That is, mechanical strain and temperature changes produce measurable electrical signals, resulting in a useful transducer material. PVDF, being a film differs from the ceramic transducer such as quartz, PZT, or barium titanate in that it is sensitive to in-plane displacement as well as the normal or out-of-plane displacement of the surface. This material also has a flat broadband frequency response which makes it ideal for use as an acoustic emission sensor.

PVDF transducers offer several advantages over ceramic element sensors. Since the material is thin and flexible, it can be easily used to fabricate transducers in complex shapes and in large sizes. These polymers have a high tolerance for mechanical stress and are thus extremely durable and can operate over much wider ranges of operating stresses. The thin films (typically 6-125 μ m) are light in weight and therefore do not perturb the mechanical response of the structure under test. In some forms, PVDF has a highly

anisotropic in-plane sensitivity, while other forms have essentially isotropic sensitivity. This characteristic could be used to produce directionally sensitive transducers. The unique attributes of PVDF open the possibilities for incorporating these transducers into a structure during its manufacture. The design and construction details of the PVDF transducers used in the ballistic impact tests described herein are shown in Fig. 4.

The main disadvantage of PVDF is its low piezoelectric output when compared to ceramics of equal size. However, this is often offset by its good acoustic impedance match when used with polymer composites. Another disadvantage in some instances is that its polymeric nature limits its use to temperature environments below 100°C. Although ferroelectric polymers have been used in many applications ranging from impact sensors to hydrophones, very little work has been done to exploit their capabilities as AE sensors. It is believed that the unique attributes of PVDF, combined with a thorough understanding of its operation and limitations, make it a promising material for ballistic impact AE applications.

Previous experience based on preliminary ballistic damage testing on the ACAP airframe at ATL, Fort Eustis, Virginia described earlier, had indicated that the PVDF transducer might be better suited for this type of application than the PCT. Therefore, a comparative evaluation of the two transducers was performed in which the transducers were mounted adjacent to each other on a composite panel. A hammer tap was used as the acoustic emission source. The results of this evaluation revealed that the PCT momentarily lost contact with the test panel during high energy events and its output signal dropped to zero. In contrast, the PVDF transducer was able to maintain contact, due to its low mass, and provided a continuous response. Based on these findings, it was decided to concentrate on the use of the PVDF transducer for the remainder of the program.

During preliminary tests designed to integrate the PVDF transducers into the overall DAES data recording system, it was determined that a voltage follower circuit needed to be developed for matching the high output impedance of the PVDF transducers (10k Ohms) with the low input impedance (50 Ohms) of the DAES system. A circuit was designed to accomplish this and successfully tested. Four units were constructed, one for each DAES input channel.

A small firing range was assembled at UTRC and a Kevlar/epoxy panel was instrumented with PVDF transducers for 0.22 cal ballistic testing. The panel was backed with sandwich stiffeners constructed of honeycomb capped with graphite/epoxy laminates. These stiffeners, when struck by a projectile, did little to alter the AE signal compared to the signals generated by impacts on the unstiffened panel portions. This series of tests was used primarily to establish instrument settings for the DAES and to check the response of the PVDF transducers. It was found during these tests that it was advisable to permanently bond the PVDF transducers to the test panel to improve the transducer response.

7.2 Task II - Prototype Damage Detection System Installation

To simulate actual hits on a full-size composite helicopter structure, attempts were made to procure the Sikorsky Aircraft Advanced Composite Airframe Program (ACAP) tool-proof airframe for use in this program. However, this proved impossible due to a conflict between its availability and program time constraints. Instead, a number of all-composite helicopter panel and structural segments were obtained from Sikorsky Aircraft. The locations of these test structures on an S-76 helicopter is diagrammed in Fig. 5 and may be described as follows:

Segment No: 1 - Main rotor forward fairing
2 - Engine/transmission support structure
3 - Rear fuselage side panel
4 - Main rotor spar
5 - Main rotor blade section
6 - Upper fuselage skin panel

Segment No. 2 is composed of graphite/epoxy; the remainder are composed of Kevlar/epoxy. As much as possible, the segments were chosen to correspond with the more critical areas of a helicopter from a survivability standpoint as elucidated earlier (See Fig. 1).

A series of PVDF strip transducers were fabricated. The sensitivity of all transducers were evaluated using a standard impact by a small ball dropped from a uniform height. Pairs of transducers with similar sensitivities were identified for use during the ballistic tests. Transducers with similar response characteristics are required to produce accurate source location and impact severity data. Further development in the design and fabrication of the PVDF transducer is desirable to reduce the disparity in sensitivity from unit to unit.

The PVDF transducers were attached to the test specimens with fast-curing epoxy. Instant or cyanoacrylate adhesives were also evaluated but did not provide adequate adhesion on the composite surface. The transducers were covered with copper tape which was connected to the system ground to provide a shield from rf interference. The transducer signal cable was attached to the line driver circuit which transmitted the acoustic signal over 75 meters of coaxial cable to the instrumentation van, a cube-type truck which housed the DAES system at the firing range. Power for the line driver was provided through a 25 volt DC bias on the signal cable. This eliminated the need to run an additional power cable to the test stand.

7.3 Task III - Ballistic Impact Tests Using Prototype Damage Detection System

Firing tests on all six composite segments were conducted at an outdoor commercial firing range (the Blue Trail Range in Wallingford, Connecticut). The test stand with each test specimen was located approximately 35 meters from the firing position and the instrumentation van was an additional ten meters behind the firing position.

The Digital Acoustic Emission System (DAES) was used to record the waveforms from the ballistic impacts. The system was configured with four independent channels each being threshold triggered by a dedicated amplifier/ trigger module. The 500 kHz digitization rate was established after a series of preliminary tests in which the frequency content of the waveforms was examined. Several shots were also fired in the preliminary tests to establish triggering levels for the amplifier modules. A record length of 6k data points (12.3 msec) was chosen to provide a record of the entire transient event. A pretrigger of 3/4k data points (1.5 msec) was used to ensure the initial portion of the waveform would be captured. The waveforms were stored on 8-in. floppy disks.

To obtain a variety of projectile velocities and impact energies in these tests, four different small arms cartridges were used. The cartridges selected were 5.6 mm, .22 cal long rifle rim fire, 7.62 mm, .30 cal carbine, 6.2 mm, .243 cal Winchester and 7.62 mm, military cal .30-06 both ball and AP types. The features of these cartridges are summarized in Table I. The impact energies shown in Table I represent a potential energy, only part of which is absorbed by the test specimen when the projectile is not completely stopped by the test specimen. The rifles used in the test were fired from a bench rest position and were fitted with accurate sights to enable the marksman to place the shots very close to the ideal point for each test.

The 5.6 mm, .22 cal long rifle cartridge represents a relatively low velocity and low energy impact. The projectile, made of solid lead, is approximately 5 mm in diameter, has a muzzle velocity of 1100 ft/sec and weighs 40 grains. (There are 7,000 grains in one pound.) Impact energy is 97.8 ft-lbs as calculated from equation 1:

(1) Energy in ft-lbs = $1/2MV^2 = WV^2/2g(7000) = WV^2/450,240$

where g = accel. of gravity = 32.16 ft/sec^2

M = projectile mass, slugs

W = projectile weight, grains

V - projectile velocity, ft/sec

The 7.62 mm, .30 cal carbine cartridge has a velocity of 1510 ft/sec with a 110 grain full jacket projectile. Impact energy is 560 ft-lbs. A cartridge of this type has a low to moderate velocity and impact energy.

A 6.2 mm, .243 cal Winchester cartridge propels a 6 mm dia. projectile weighing 85 grains at 3300 ft/sec. Impact energy is 2055 ft-lbs. This is a high velocity, moderately high impact energy cartridge.

For high velocity and high impact energy, two types of 7.62 mm, cal .30-06 ammunition were used: standard ball and armor-piercing (APM2). The velocity and energy of these two 7.62 mm dia., 167 grain projectiles are identical, 2700 ft/sec and 2800 ft-lbs, respectively.

The velocity and energy data represent the conditions at the muzzle of the rifle. The impact point of approximately 35 meters down-range results in no more than a 10% decrease in these values at that range.

The test specimens used for ballistic testing were acquired from Sikorsky Aircraft and represent a wide variety of composite structures used in helicopter airframes. The test specimens and the number and types of ballistic impacts on each are summarized in Table II. A listing of all hits on the test specimens showing responding transducers, hit positions and the resulting signal peak RMS values is delineated in an Appendix to this report. The significance of the RMS analysis technique is elucidated later in this report under the description of test results for segment No. 5.

7.3.1 Test Results - Segment No. 1

Figures 6 and 7 show front and rear close-up views of the hits on segment No. 1. Note the positions of the transducers shown in Fig 7. Transducers A and B are located on spars or stiffeners while transducer C is affixed to the panel skin. Typical resulting acoustic waveforms are shown in Figs. 8 and 9. As expected, the peak amplitude and peak RMS value are considerably greater for the on-spar hit (Fig. 8) than for the off-spar hit (Fig 9). The very low output of transducer C in both cases probably results from the hits being located relatively far away on the other side of the central spar.

7.3.2 Test Results - Segment No. 2

Figure 10 shows a front view of test panel segment No. 2, part of the helicopter engine/transmission support structure. The test panel is basically a box structure with 1/4 in. thick walls. A horizontal plate at the midsection of the interior of the box connects the front and back surfaces, and provides a path for AE generated on the back surface of the box to travel to the front surface. The PVDF transducers were attached to the front surface directly over the locations where the horizontal midsection plate attached to the front surface. Thus, it is possible that a second burst of AE was generated by the impact of the projectile with the back surface.

Figures 11 and 12 show typical transducer output waveforms for segment No. 2. For some of the ballistic impacts on segment No. 2, the segment was physically located behind segment No. 3. (See listing of hits in the Appendix.) Thus, the projectile had to pass through segment No. 3 prior to impacting segment No. 2. Figure 11 shows such a case. It is to be expected that there would be an extrusion or flattening of the projectile as it passed

through segment No. 3. This would result in a much greater generation of acoustic energy by the enlarged projectile in segment No. 2 than for the case when the projectile passes through cleanly. This explains the greater acoustic emission for the impact by the 5.6 mm projectile (Fig. 11b) versus that by the 7.62 mm projectile (Fig. 12b).

Acoustic emission signals below 50 kHz are susceptible to interference from various sources such as mechanical vibrations and airborne sound. A study, therefore, was conducted on segment No. 2 to assess the ability of the system to detect AE signals above 80 kHz. For these tests a band-pass filter was inserted into the signal path of one channel (transducer C) immediately before the amplifier modules. The filter was adjusted to pass signal frequencies from 80 kHz to 1.0 MHz. The second channel of the data acquisition system (transducer D) remained unchanged. Tests were conducted with 7.62 mm, cal .30-06 ammunition.

A typical waveform for the filtered and unfiltered signal is shown in Fig. 12. The ratio of the peak RMS values for the unfiltered vs the filtered signals for this case is 3.3. The amplitude ratio is approximately 3.0. In general, the amplitudes of the unfiltered waveforms are larger than the filtered by a factor of 3 to 5 depending on the relative distance of the impact to each transducer. The waveforms from this test exhibited two bursts of AE energy spaced 300 μsec apart. The second AE burst is more distinct on the high frequency waveforms and is generally larger in amplitude than the initial burst. Post-test examination of the beam revealed that the front surface entrance and exit holes were very clean. However, the exit damage from the back surface was more severe in that there was a larger penetration area which exhibited broken fibers and delamination. This was caused by extrusion or flattening of the projectile as it penetrated the front surface. Thus, it is to be expected that the AE generated from the back surface impact would be larger in amplitude than the front surface impact. However, the acoustic waves had to travel a longer distance through the structure and thus were attenuated more than the AE energy from the front surface impact. Therefore, the relative amplitude between the front and back surface signals will not correspond exactly to the relative difference in the severity of damage between these two locations. However, this does explain why the back surface AE burst can be larger than the front surface AE burst.

Further, calculations show that the 300 μsec separation of the two bursts corresponds to a projectile velocity of 2014 ft/sec or 75% of the muzzle velocity. This value is reasonable given that the projectile has already penetrated a 1/4 in. thick graphite/epoxy wall.

It was concluded that the second AE burst seen in Fig. 12a resulted from the impact of the projectile with the back surface of the structure. Furthermore, it was demonstrated that there is sufficient AE energy in the 80 kHz to 1 MHz frequency range to detect a ballistic impact on both surfaces of the structure. In a general application the attenuation increases as the

frequency of the AE signal increases. This attenuation effect is magnified by the nonhomogeneous make-up of composites. Therefore, transducer spacing on a structure will be required to be closer for a high frequency detection system than that required for a low frequency system. The high frequency system, however, would exhibit better noise immunity.

7.3.3 Test Results - Segment No. 3

Photographs of test panel segment No. 3, a rear fuselage side panel are shown in Figs. 13 and 14. Typical transducer output waveforms are shown in Figs. 15 and 16. Note again that a comparison of the two figures indicates a greater generation of acoustic energy indicating a greater absorption of impact energy when the test specimen is penetrated by the much slower 5.6 mm projectile than by the 6.2 mm Winchester projectile. In Fig. 16, the peak signal amplitude is much greater for the on-spar hit (part b) than for the off-spar hit (part a) even though the peak RMS values are nearly identical (but very low, indicating a small amount of energy absorption).

7.3.4 Test Results - Segment No. 4

Segment No. 4, a main rotor spar, is shown in the photograph in Fig. 17. The waveforms shown in Figs. 18 and 19 indicate a very high impact energy absorption for the carbine and military 7.62 mm ammunition (Figs. 18a, 18b, and 19a). Figure 17 also gives an indication of the large amount of damage caused by these impacts. The impact energy absorption for the 5.6 mm projectile (Fig. 19b) is considerably less. Note also that the signal peak RMS value is much greater for transducer A in Fig. 18 than for transducer B. This is indicative of the greater acoustic transmission path length to transducer B, since the hit was located near transducer A.

7.3.5 Test Results - Segment No. 5

Test specimen No. 5 consists of a section of main rotor blade and is shown in the photograph in Fig. 20. The main purpose of the ballistic tests on panel No. 5 was to differentiate between an impact on the spar from an impact off the spar (in an area containing a honeycomb structure), i.e., between an impact in an important structural area versus a non-structural area. One PVDF transducer, labeled A, was attached to the blade surface directly over the centerline of the spar. The second transducer, labeled B, was attached to the blade surface over the honeycomb reinforcement adjacent to the spar. It was expected that the response of each transducer would be different for off-spar and on-spar impacts. The ballistic impacts were divided into five groups which correspond to the five impact sites shown in Fig. 20.

The waveforms for segment No. 5 shown in Figs. 21 and 22 indicate considerably greater energy absorption for the spar hit (Fig. 21) than for the off-spar hit (Fig 22).

An RMS analysis technique was chosen to investigate the data from hits on this segment. The computation of the RMS amplitude-versus-time signal provides a measure of the signal energy and this is presumably an indicator of damage severity. An RMS algorithm which operates on the digitized waveforms is implemented on the DAES system. A plot of the amplitude RMS vs. time is obtained for each waveform and the peak value is recorded. Figure 23 shows two examples of these plots. Since the absolute amplitude of the AE signal, and also the resulting peak RMS, is significantly affected by the source to sensor distance due to attenuation, the amplitude alone cannot provide an indication of the impact energy. It is more appropriate to use a ratio of the amplitudes of the signals from two transducers as a method of determining impact energy since the ratio is more distance insensitive.

For a given ballistic shot, the peak RMS values of the waveform from transducer A and from transducer B were calculated. The ratio of the peak RMS for transducer A to the peak RMS for transducer B was then calculated. The results for all hits on test panel No. 5 are shown in Table III and demonstrate a significant change in the ratio between any off-spar hit and any on-spar hit. The analysis was continued by combining the ratios for all impacts off the spar into one group and all the impacts on the spar into another group. The mean ratio for each group was then calculated and the results are shown in Table III. One ratio represents all of the off-spar hits and another ratio represents all of the on-spar hits. The average ratio of the transducer A/transducer B ratios for on and off spar hits is 12.9. Because the distances of the impacts to the two sensors is approximately equal, this average signal ratio of 12.9 is indicative only of impact severity not of transmission losses. Hence, the energy ratio technique provides an accurate differentiation between on-spar hits and off-spar hits for all tests conducted on the blade section. The test segment was not sufficiently large to evaluate the effect large ballistic impact source to sensor distances have on the accuracy of this technique.

7.3.6 Test Results - Segment No. 6

Acoustic emission source location is a method whereby an array of transducers is used to detect and locate a transient AE event. For a given array of transducers, the time difference of arrival (Δt_1, Δt_2, etc.) is measured by starting a clock when the first transducer detects the event. For each of the other transducers, the time t_n is defined as the clock reading when that transducer detects the event. Thus, ΔT for the first-hit transducer is defined as zero.

For two transducers on a planar surface, points of equal Δt's form a series of hyperbolas. (For a more complete discussion see Ref. 2.) The pattern of hyperbolas for a square array of four transducers is shown in Fig. 24. It can be shown that the loci of equal Δt's forms an approximate x-y coordinate system. As shown in Fig. 24, the origin of this system is at the center. Note that the accuracy decreases near the edge of the grid. Thus a simple equation can be used to compute the x-y location given the signal detection time for each of the four transducers:

$$x = K\,(\Delta t_{ca} + \Delta t_{bd}) \tag{2}$$

$$y = K\,(\Delta t_{ca} + \Delta t_{bd}) \tag{3}$$

where

$$\Delta t_{ca} = t_c - t_a \tag{4}$$

$$\Delta t_{bd} = t_b - t_d \tag{5}$$

In these equations, K is a constant which accounts for the velocity of sound in the material. It is generally determined through calibration tests.

A 20-inch square grid was constructed on test panel segment No.6 with a PVDF transducer at each corner as shown in the photograph of segment No. 6 in Fig 25. The origin of this coordinate system was at the lower left. The data acquisition system was configured such that one arbitrarily chosen channel would trigger the three other digitizers simultaneously when it detected an AE event. Since the beginning of the event was the only part of interest, the amplifiers were set at their maximum gain of 20 dB. This allowed the initiation of the event to be more easily detected. Time resolution was enhanced by operating the digitizers at a 4 MHz sampling frequency.

Ballistic tests were performed on this panel using military 7.62 mm, cal .30-06 ammunition. The x-y location of each impact was recorded along with the waveform from each of the four transducers.

The analysis of this data was performed by visually inspecting each waveform. The time at which the event started was then recorded for each of the four waveforms for each ballistic test. Since all four channels were triggered simultaneously, the Δt values for each channel were simply computed by subtracting the start time of the first-hit transducer from the start times of the other three. Thus, for each of the tests, the Δt associated with each transducer was found.

A computer program was written using the previously described algorithm which provided the x-y location as an output from the Δt inputs. The data from three of the six tests along with their known x-y positions were used in an iterative procedure to determine the best-fit value of the constant K in equations 2 and 3. Once this was completed, the x-y position for each of the six tests was computed. The results are shown in Fig. 26. Good accuracy was achieved with a mean radial error of 1.3 in. which is approximately seven percent of the array edge distance. The maximum error was only 1.9 in. which is less than ten percent of the array edge distance.

7.3.7 Circuitry Required for Flight Implementation

All of the above data were recorded and analyzed on large-scale test and computer equipment in non real-time. It is technically feasible, however, to miniaturize the electronics required for these calculations for the next generation data system. Figure 27 shows a block diagram incorporating a four transducer array and a circuit representative of the hit location (time difference) and feature extraction (impact severity analysis) functions. It is anticipated that these functions could be contained within a package of VLSI (very large scale integrated) circuit chips. The feature extraction function could be located on a single VLSI circuit chip as indicated by the block diagram in Fig. 28. A minimum of two sensors is shown in the diagram in Fig. 28 to implement the RMS ratio method described previously.

The components and circuitry required to functionally implement the signal processing function depicted in Figs. 27 and 28 are well within the current state of the art. The RF amplifications and RMS functions can be accomplished with existing hybrid circuitry which is adaptable to VLSI packaging. The ratio and time difference calculations could be accomplished with a single chip microprocessor. Both circuits would require very low power and could easily operate on existing aircraft power supplies. It is anticipated that the final flightworthy sensor/signal processing package would be very lightweight and cost effective. The actual number of sensor/signal processing packages required per aircraft is variable, but is expected to be less than 12.

8.0 REFERENCES

1. Carper, C. H. Jr.: "Combat Damage Assessment." Applied Technology Laboratory, US Army Research and Technology Laboratories (AVSCOM), presented at 51st AGARD Structures & Materials Panel/Specialists Meeting (AGARD CP 297), Aix-en-Provence, France, Sept. 1980.

2. Barsky M. and Hsu N. N: "A Simple and Effective Acoustic Emission Source Location System." Materials Evaluation, Vol. 43, No. 1, Jan. 1985, pp. 108-110.

Table I - Summary of Projectile Features

Projectile				Projectile Weight Grains	Muzzle Velocity ft/sec	Impact Energy ft-lbs
No.	Cal.	mm	Description			
1	.22	5.6	Rim-fire	40	1100	97.8
2	.243	6.2	Winchester	85	3300	2055
3	.30	7.62	Carbine	110	1510	560
4	.30-06	7.62	Ball	168.5	2700	2780
5	.30-06 APM2	7.62	Armor-piercing	168.5	2700	2780

Table II - Summary of Test Specimens and Ballistic Impacts

Composite Segment No.	Description	Material	Ref. Fig. Nos.	No. of Hits				
				5.6 mm	6.2 mm	7.62 mm Carbine	7.62 mm Ball	7.62 mm APM2
1	Main rotor forward fairing	Kevlar/ epoxy	6-9	9				
2	Engine/transmission support structure	graphite/ epoxy	10-12	7	4			
3	Rear fuselage side panel	Kevlar/ epoxy	13-16			5		
4	Main rotor spar	Kevlar/ epoxy	17-19	7		4	3	1
5	Main rotor blade section	Kevlar/ epoxy	20-23	24				
6	Upper fuselage skin panel	Kevlar/ epoxy	25-26				13	

Table III - Peak RMS Signal Values, Off-Spar vs On-Spar Hits

Segment 5

Type of Hit	Peak RMS Signal Values			
	Transducer A	Transducer B	Ratio A/B	Mean Ratio A/B
Off-spar	7.18	24.57	0.29	
	5.48	29.01	0.19	
	9.79	39.34	0.24	0.24
	9.24	41.92	0.22	
	6.93	30.88	0.22	
On-spar	225.5	129.7	1.74	
	216.7	95.8	2.26	
	160.2	123.8	1.29	
	211.3	131.1	1.61	3.04
	818.5	123.0	6.65	
	792.0	274.4	2.89	
	657.7	106.0	6.21	
	257.6	155.7	1.66	

$$\text{Mean Peak RMS Signal Ratio,} \quad \frac{\text{On-Spar}}{\text{Off-Spar}} = 12.9$$

SYSTEM IMPLEMENTATION

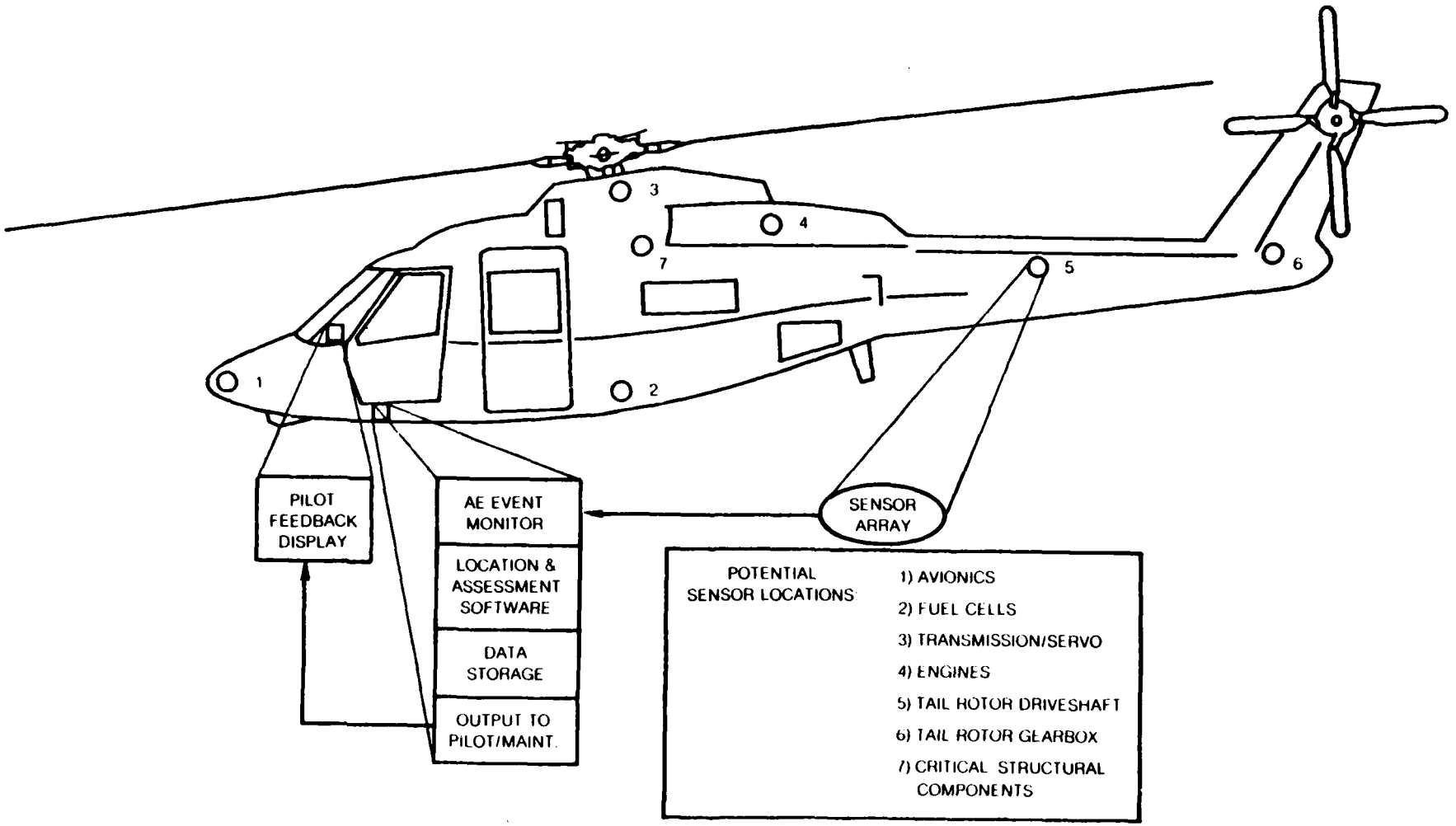

85-11-28-1

FIG. 1

DIGITAL ACOUSTIC EMISSION SYSTEM

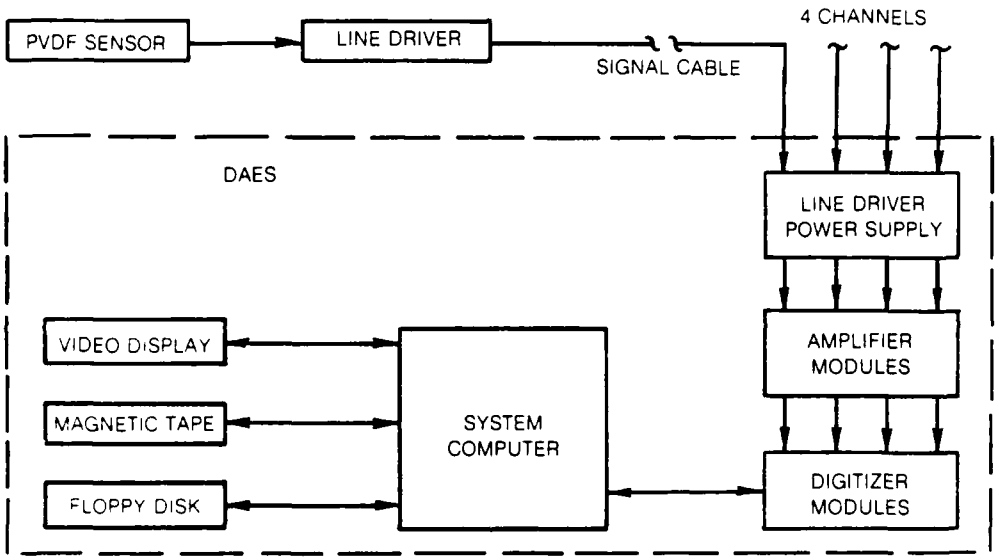

85-11-28-2

POINT CONTACT TRANSDUCER (PCT) CONSTRUCTION

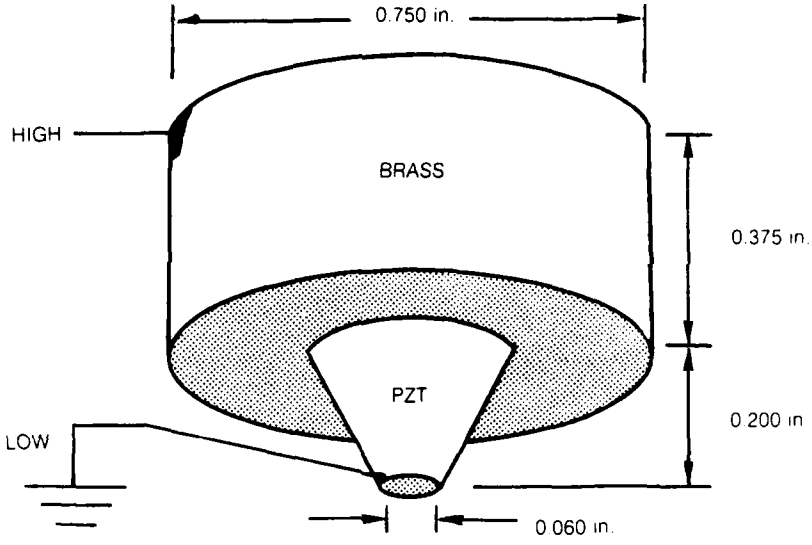

85-11-28-3

POLYVINYLIDENE FLUORIDE (PVDF) TRANSDUCER CONSTRUCTION

A) TOP VIEW

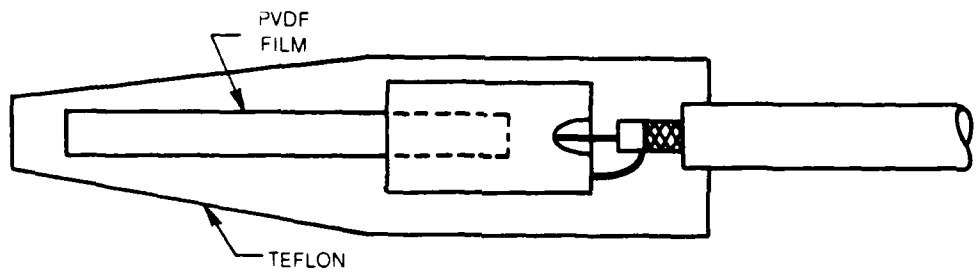

B) SIDE VIEW

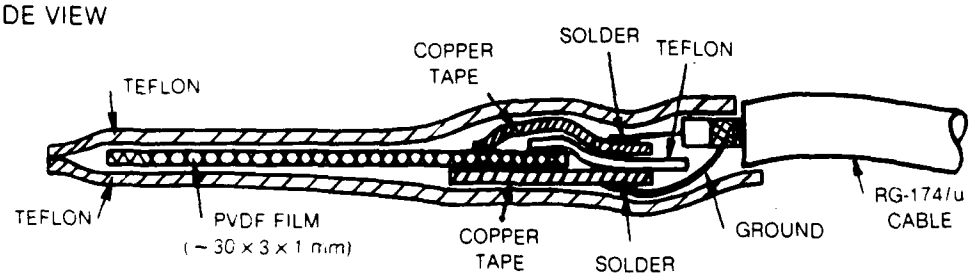

85-11-28-4

FIG. 5

TEST SPECIMEN LOCATIONS ON HELICOPTER

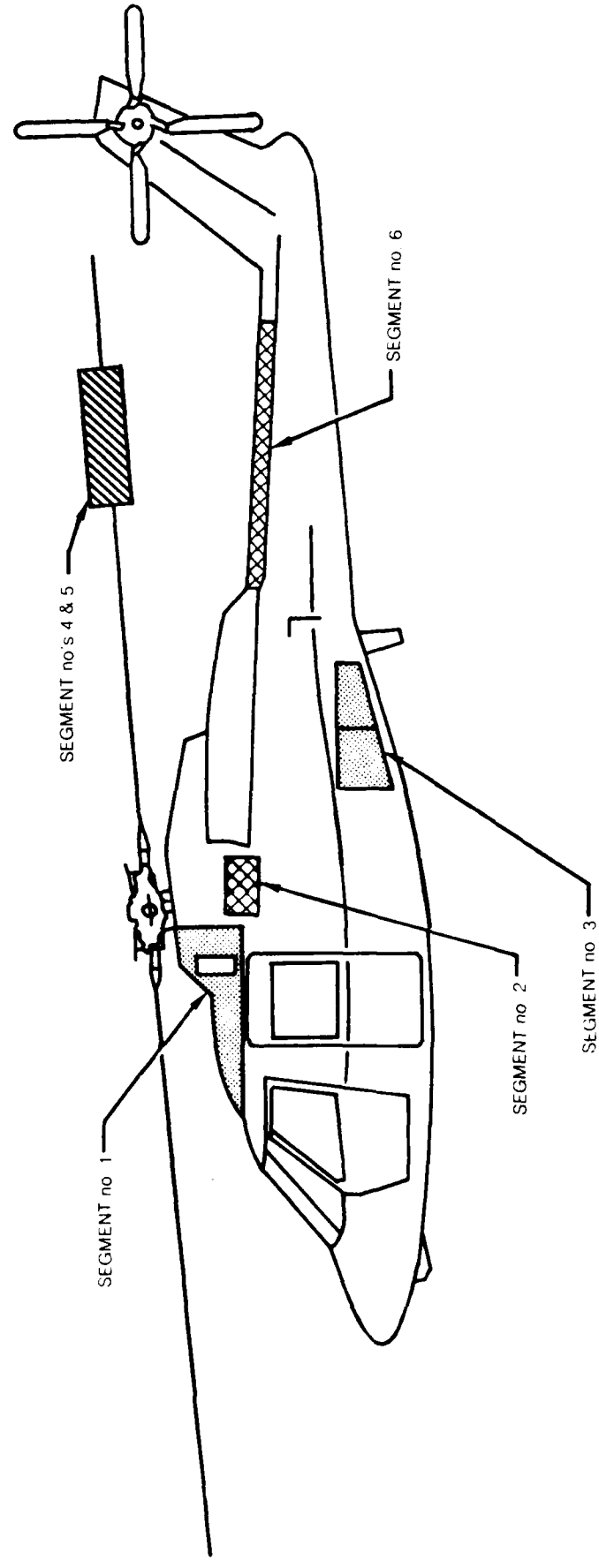

85-11-28-5

FIG. 6

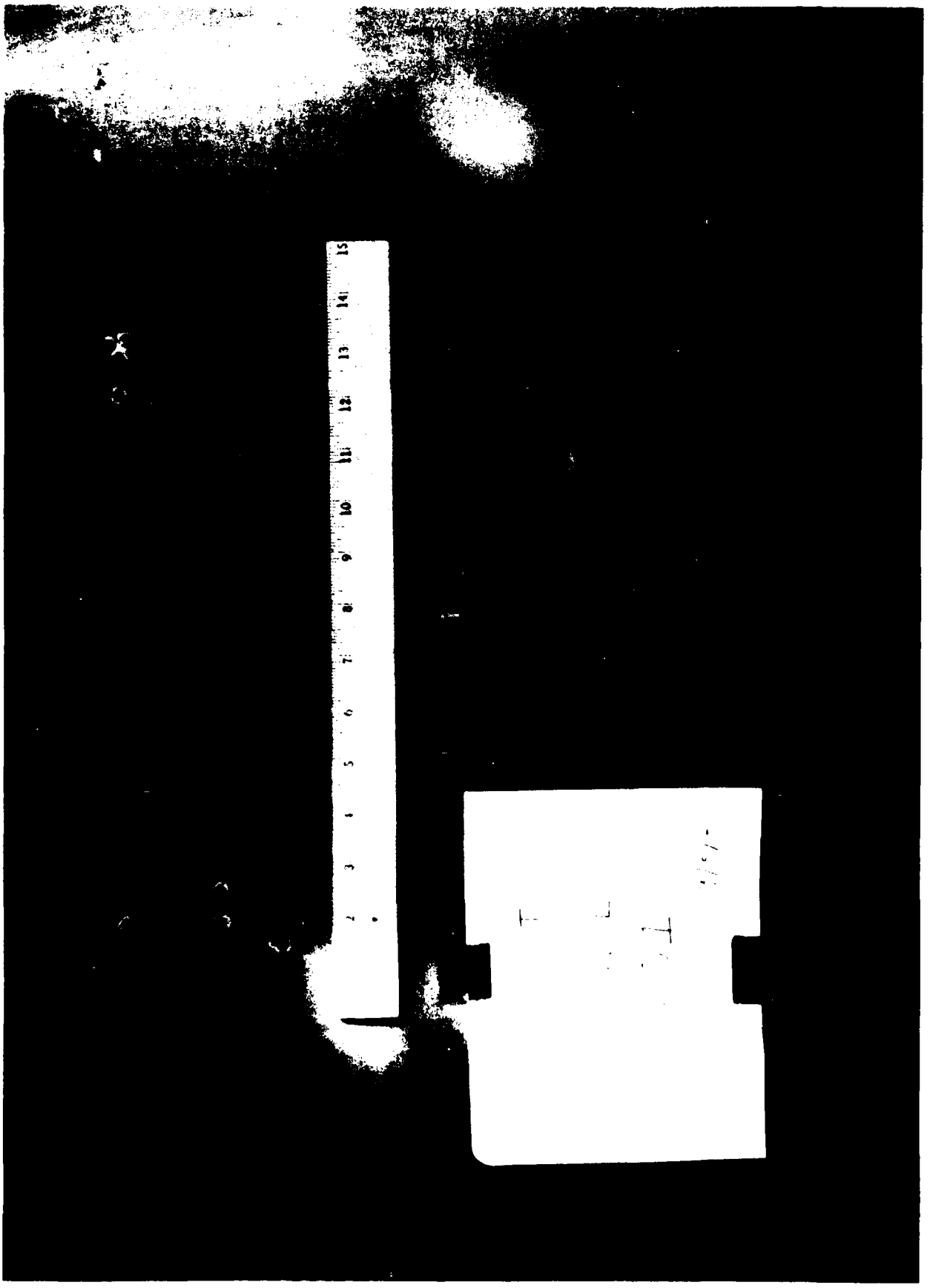

TEST PANEL SEGMENT NO. 1 — FRONT VIEW

85-11-28-26

FIG. 7

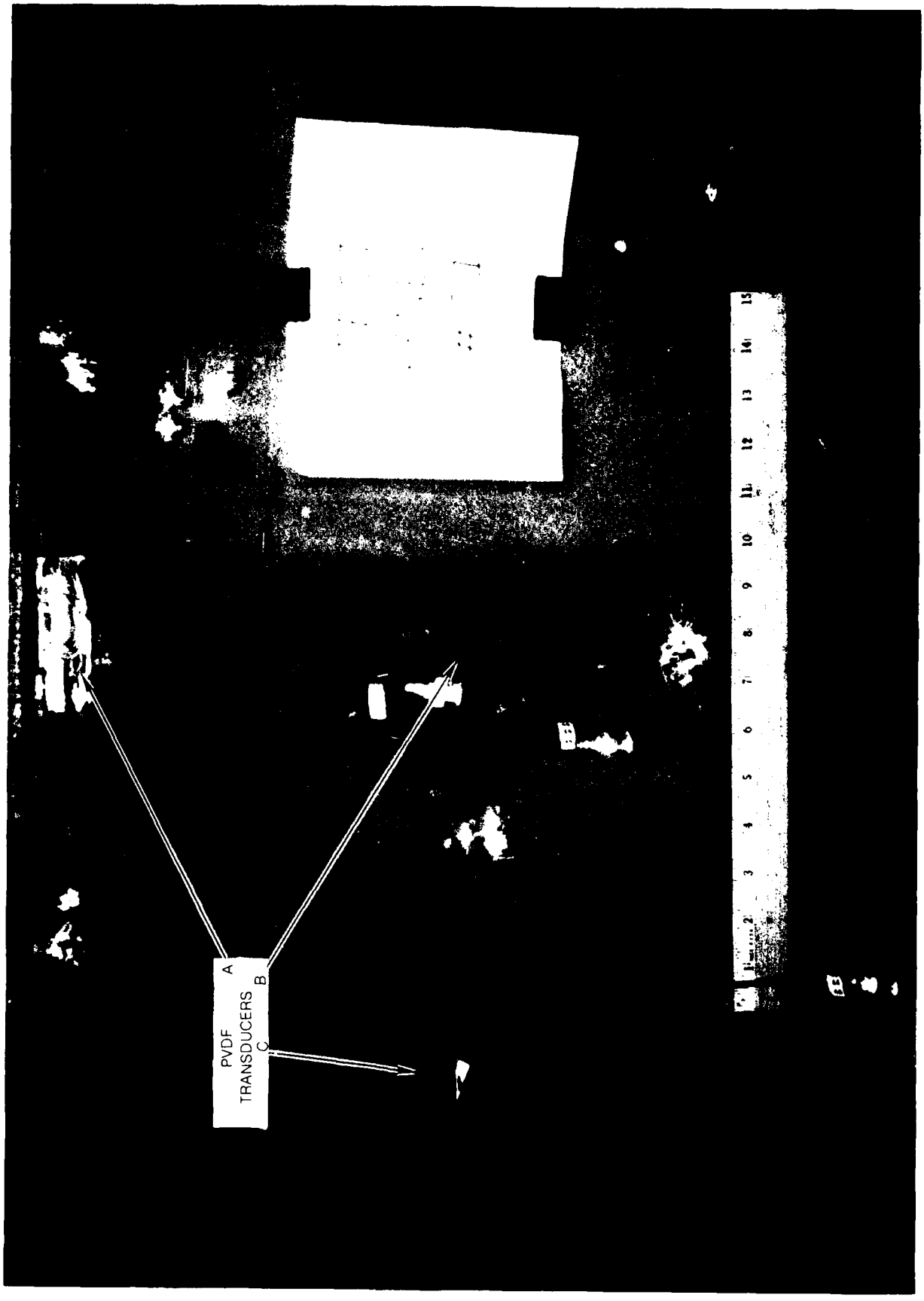

TEST PANEL SEGMENT NO. 1 — REAR VIEW

85-11-28-25

TYPICAL WAVEFORMS — SEGMENT NO. 1

HIT: ON SPAR
5.6 mm AMMO

A) TRANSDUCER A OUTPUT

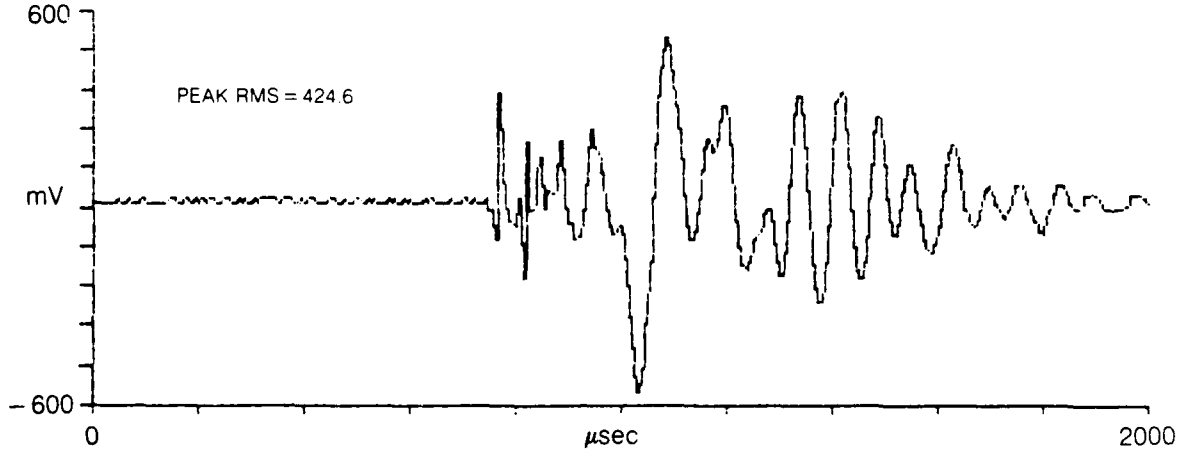

B) TRANSDUCER C OUTPUT

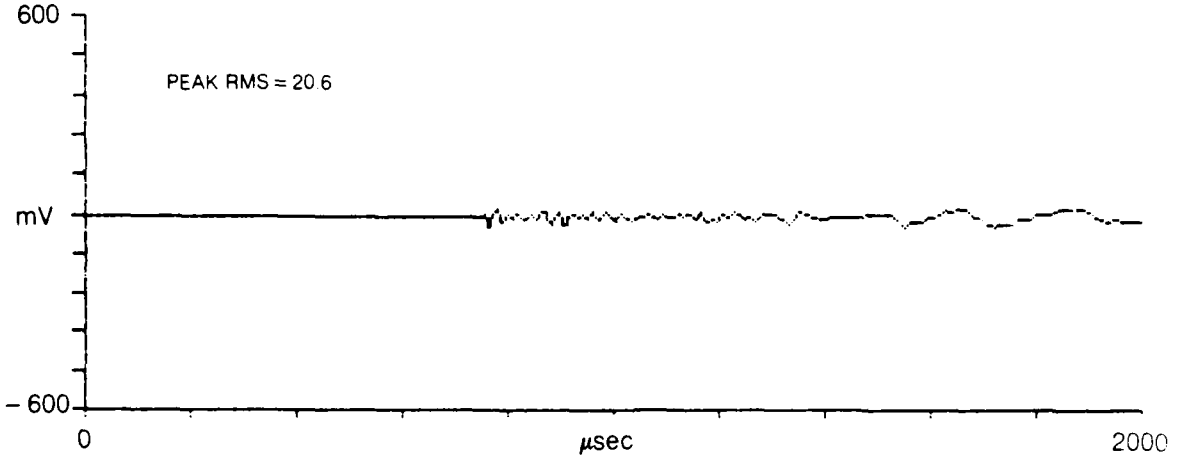

85–11–28–6

TYPICAL WAVEFORMS — SEGMENT NO. 1

HIT OFF SPAR
5.6 mm AMMO

A) TRANSDUCER A OUTPUT

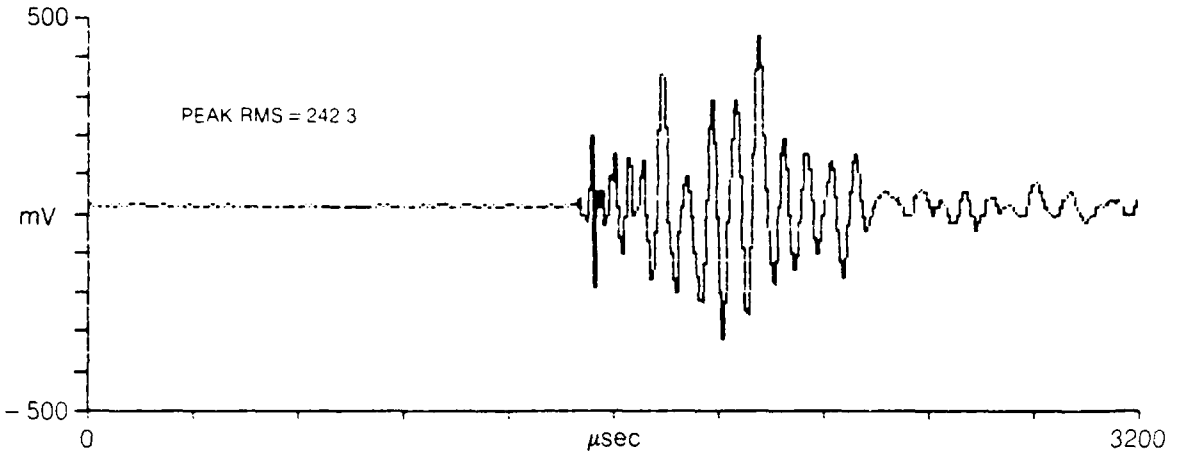

B) TRANSDUCER C OUTPUT

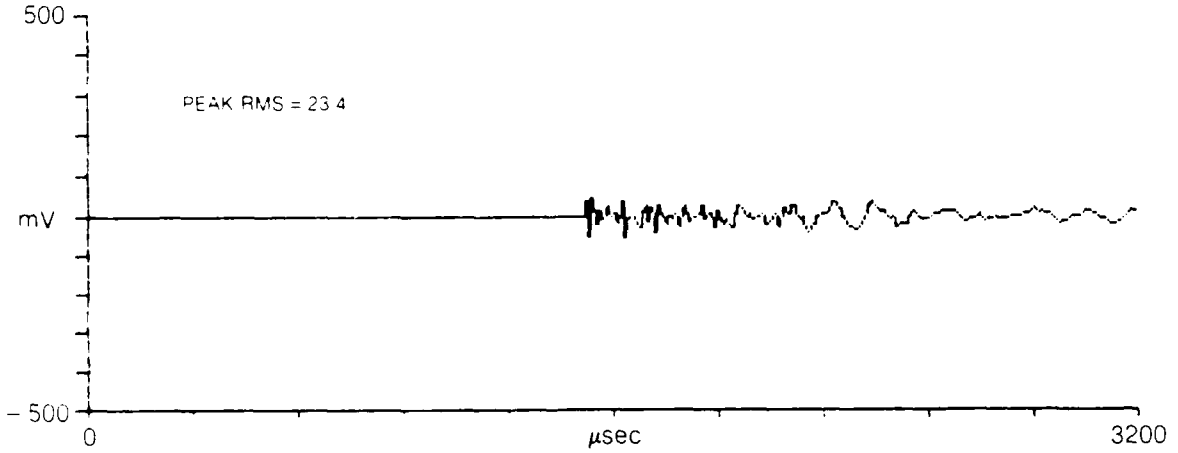

85–11–28–7

FIG. 10

TEST PANEL SEGMENT NO. 2 — FRONT VIEW

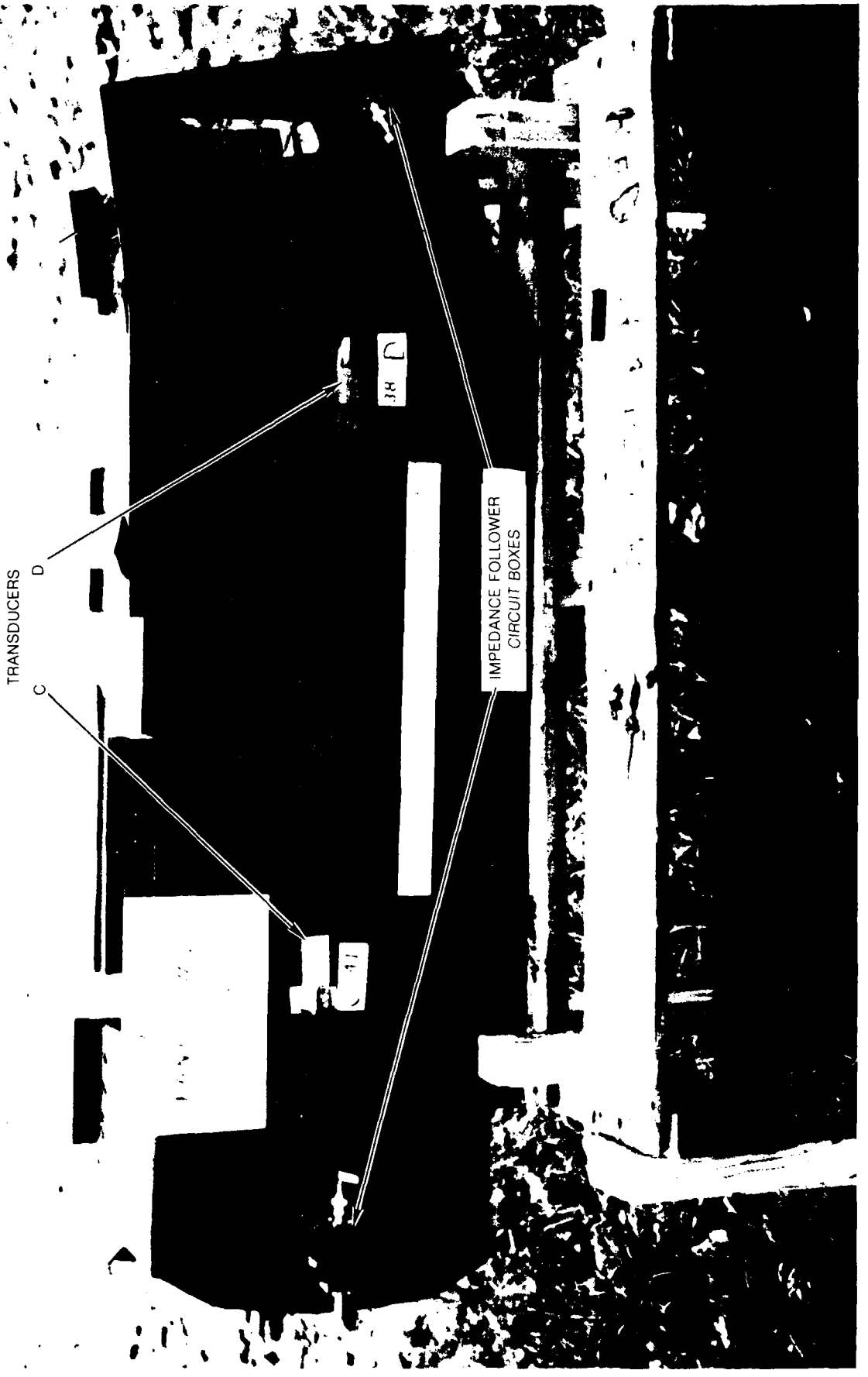

85-11-28-24

TYPICAL WAVEFORMS — SEGMENT NO. 2

HIT: LOWER MIDPOINT OF SEGMENT
5.6 mm AMMO

A) TRANSDUCER C OUTPUT

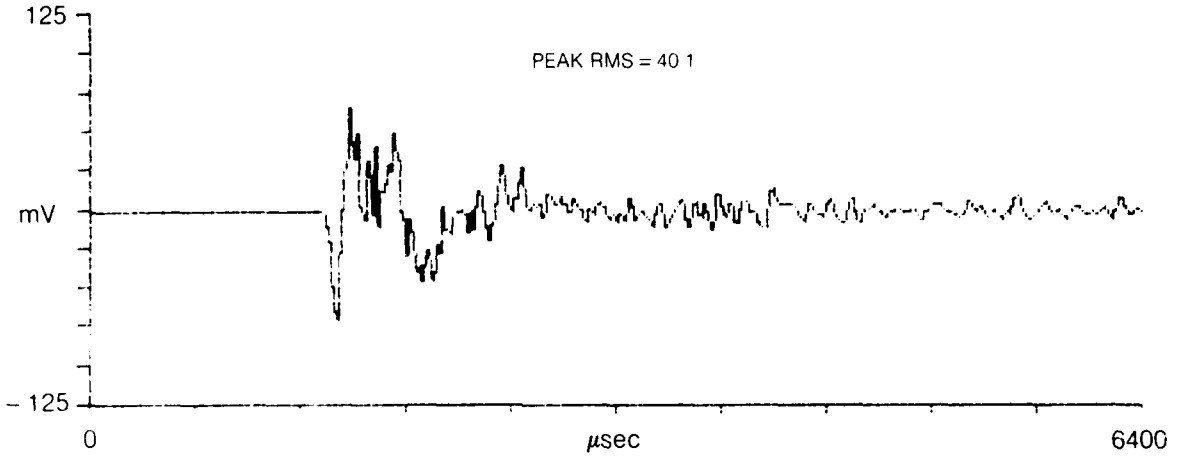

B) TRANSDUCER D OUTPUT

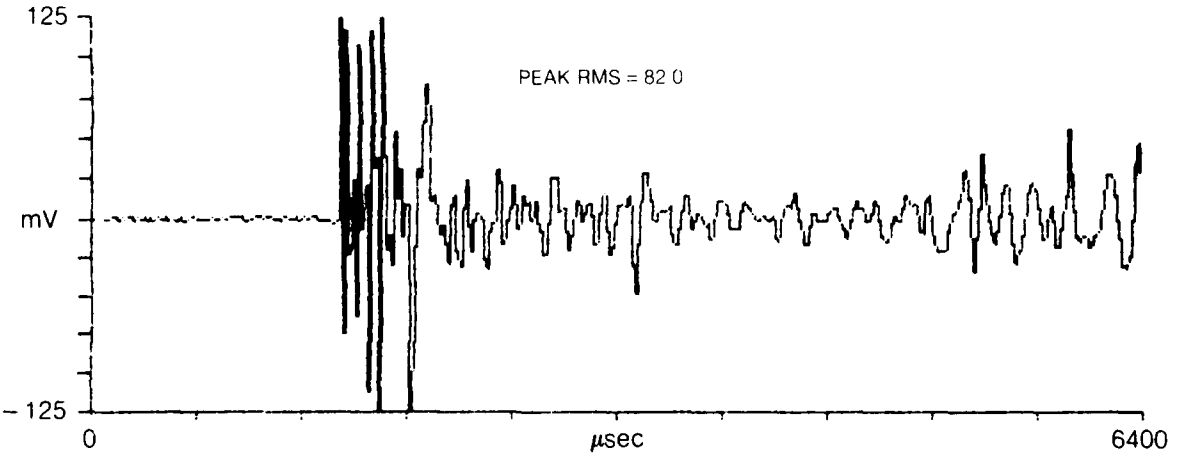

85–11–28–8

TYPICAL WAVEFORMS — SEGMENT NO. 2

HIT MIDPOINT OF SEGMENT
7.62 mm BALL AMMO

A) TRANSDUCER C OUTPUT (FILTERED)

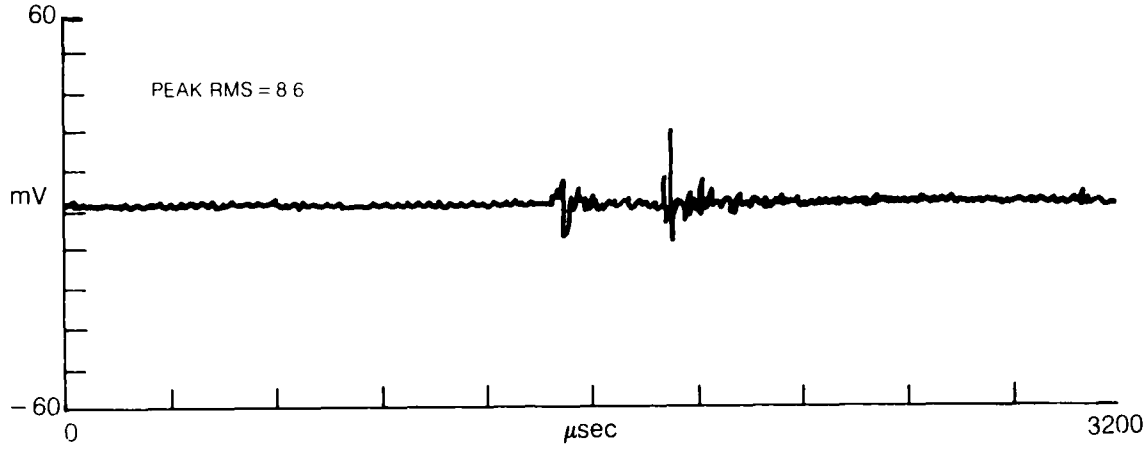

B) TRANSDUCER D OUTPUT (UNFILTERED)

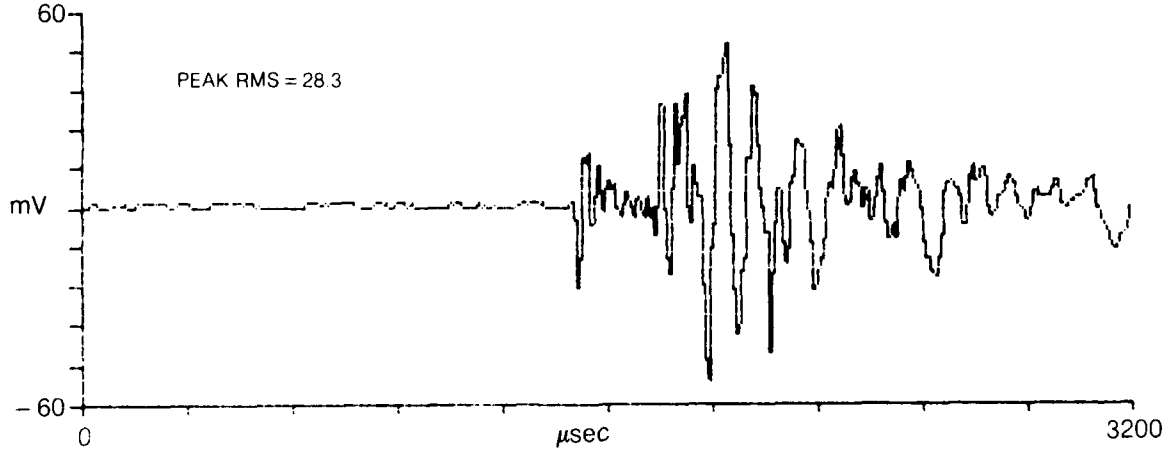

85–11–28–9

FIG. 13

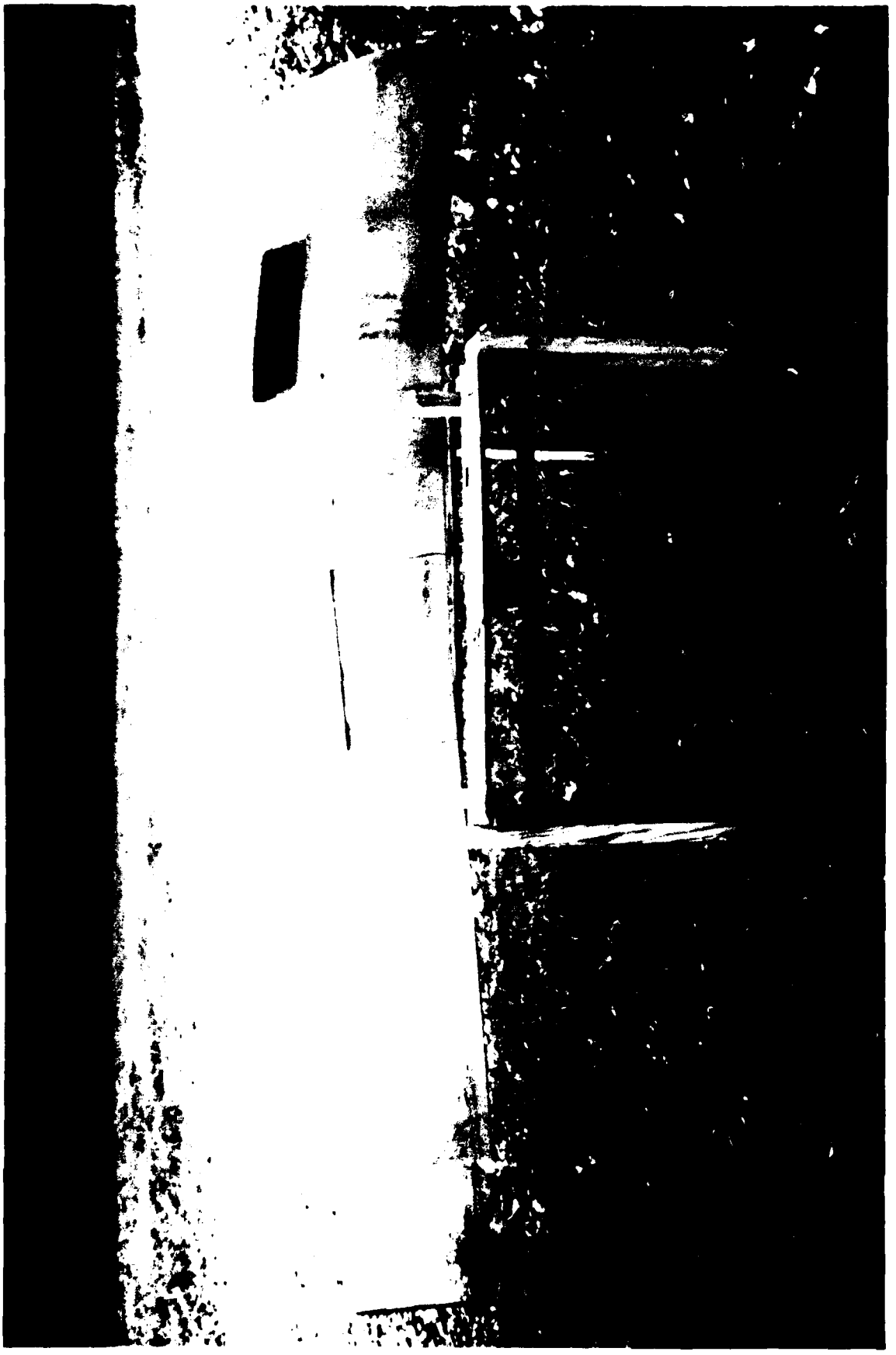

TEST PANEL SEGMENT NO. 3 — FRONT VIEW

85-11-28-23

FIG. 14

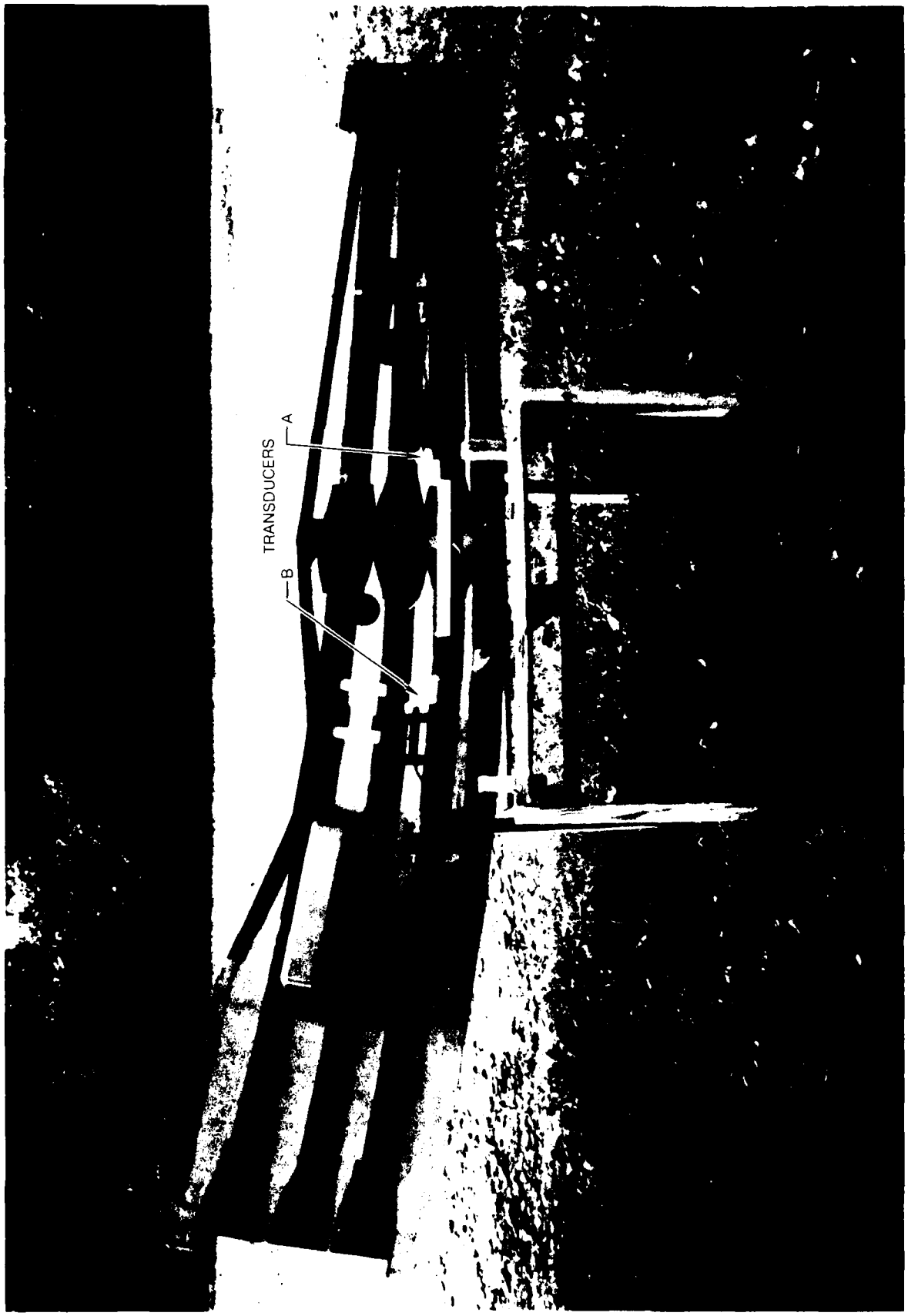

TEST PANEL SEGMENT NO. 3 — REAR VIEW

85-11-28-22

TYPICAL WAVEFORMS — SEGMENT NO. 3

HIT: POSITION 2 — UPPER MIDPOINT OF A & B
5.6 mm AMMO

A) TRANSDUCER A OUTPUT

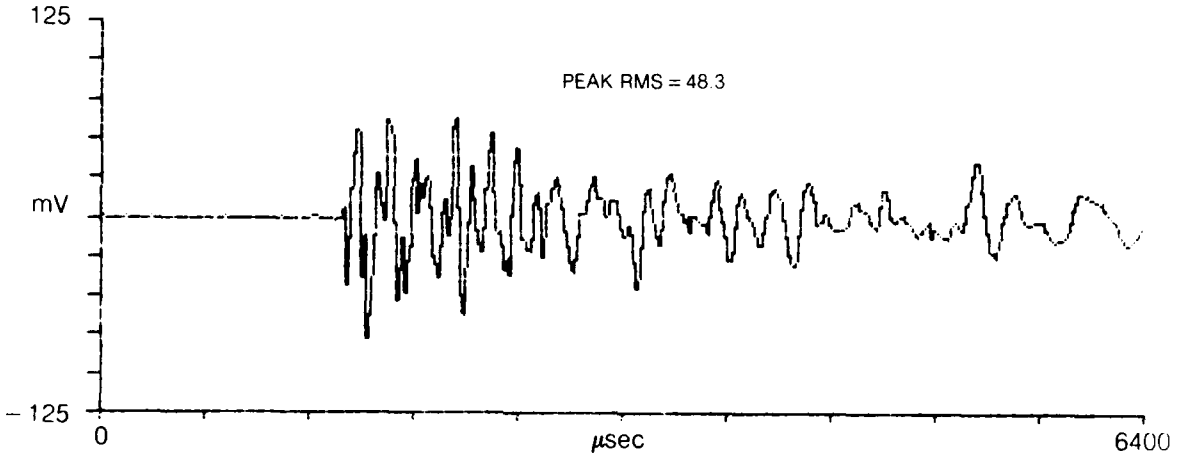

B) TRANSDUCER B OUTPUT

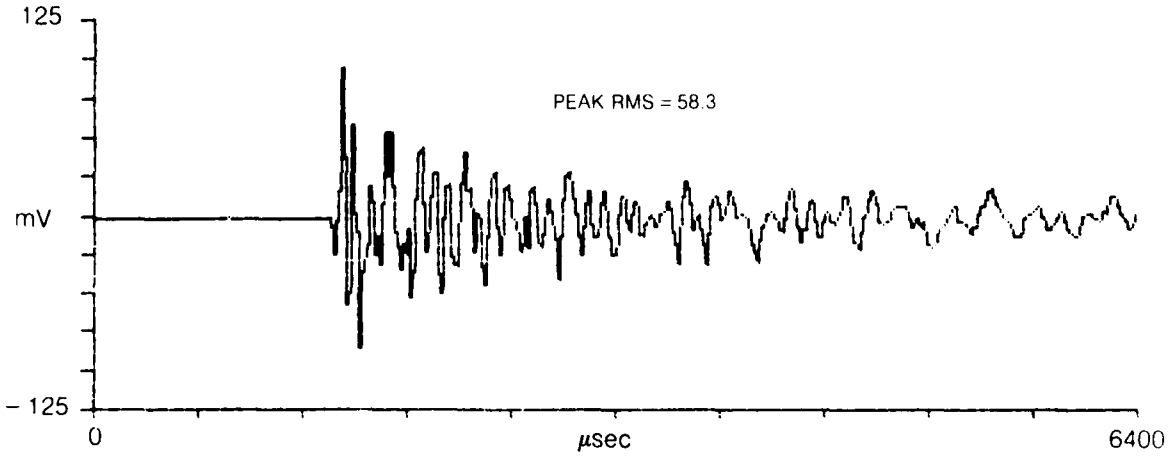

85–11–28–10

FIG. 16

TYPICAL WAVEFORMS — SEGMENT NO. 3

TRANSDUCER A OUTPUT
6.2 mm WINCHESTER AMMO

A) HIT: OFF SPAR

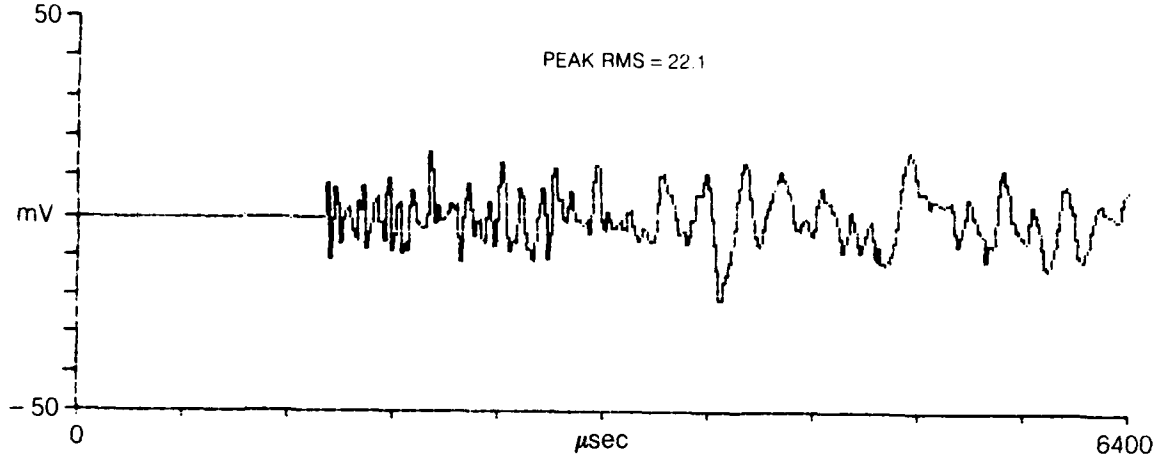

B) HIT: ON SPAR

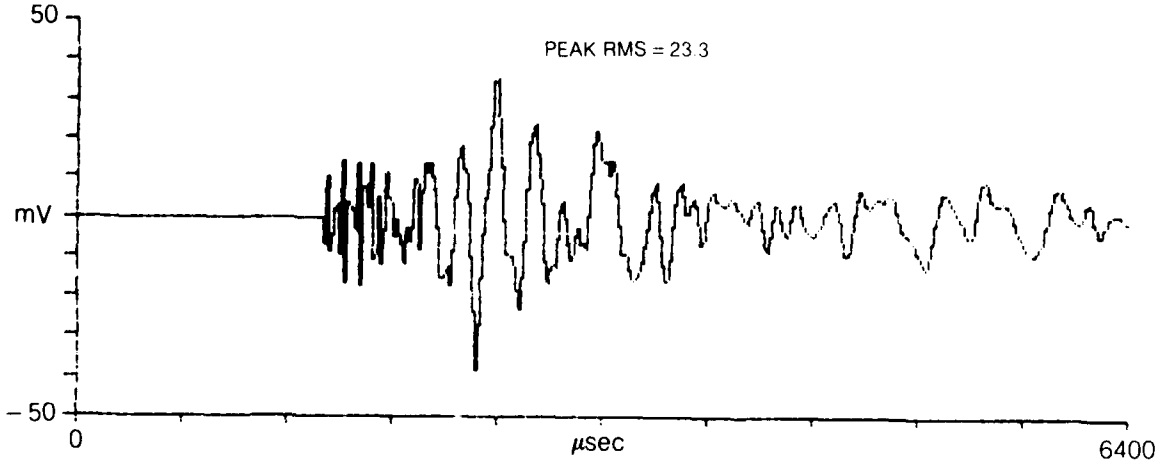

85–11–28–11

FIG. 17

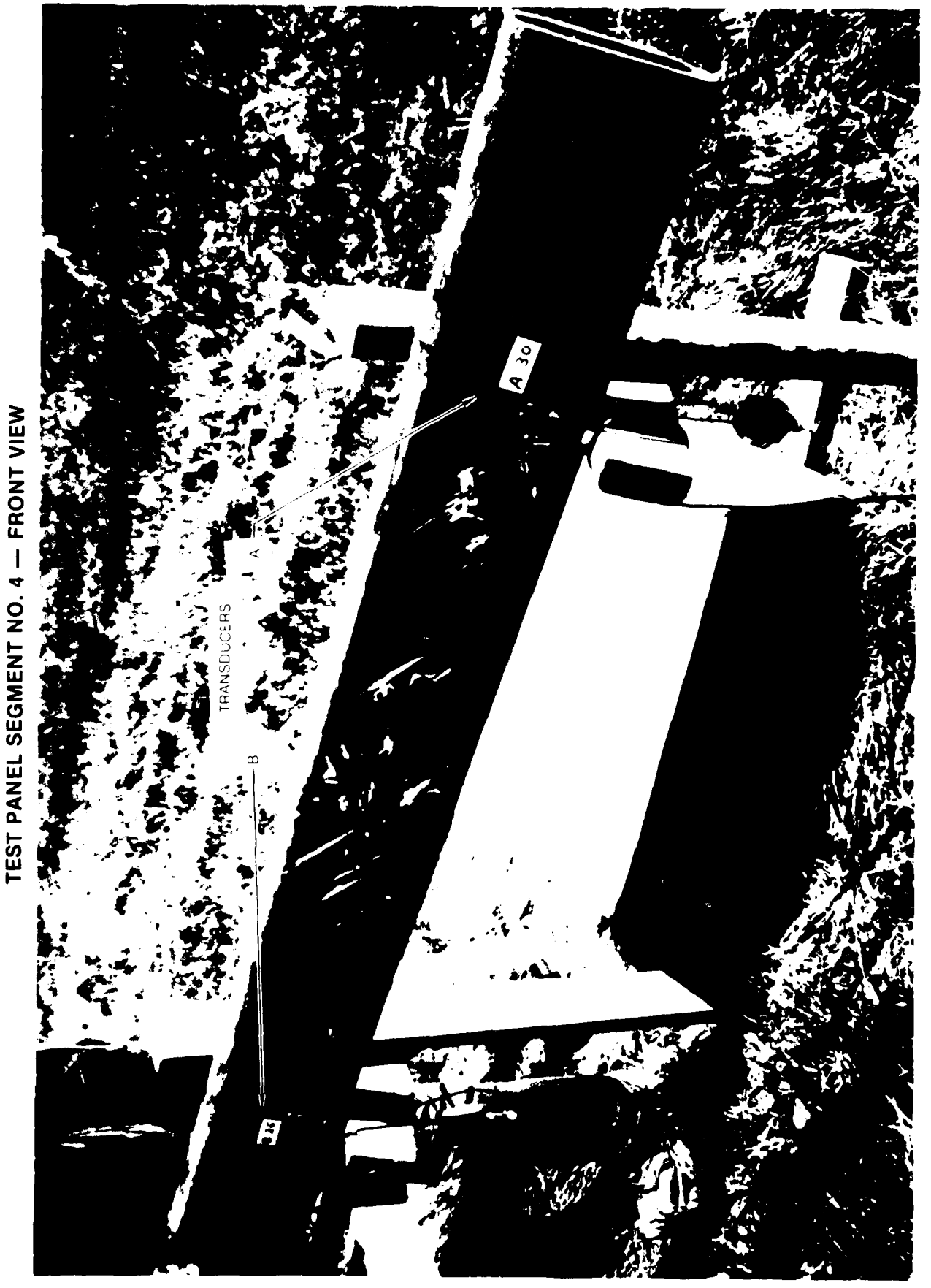

TEST PANEL SEGMENT NO. 4 — FRONT VIEW

85-11-28-21

TYPICAL WAVEFORMS — SEGMENT NO. 4

HIT NEAR TRANDUCER A
7 62 mm CARBINE

A) TRANSDUCER A OUTPUT

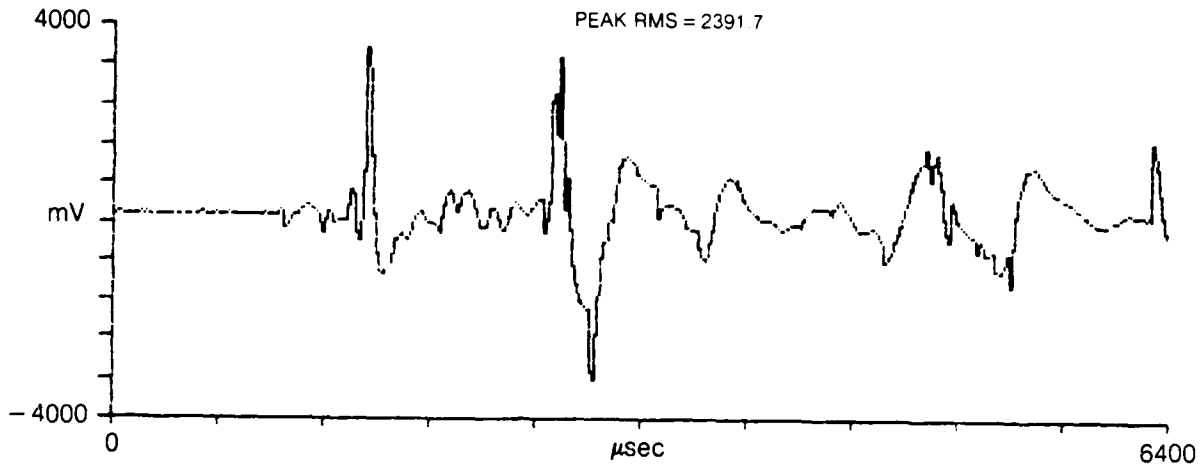

B) TRANSDUCER B OUTPUT

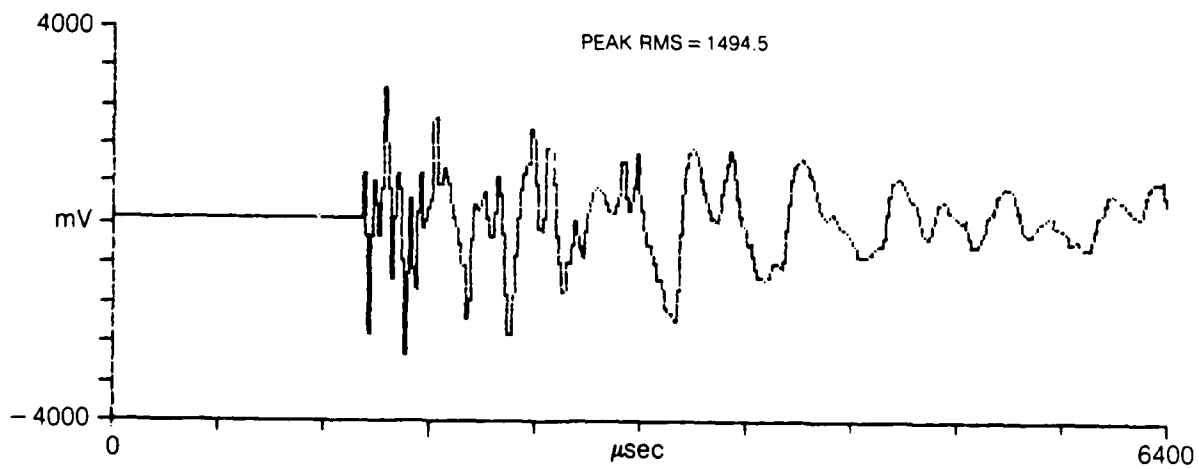

85–11–28–12

TYPICAL WAVEFORMS — SEGMENT NO. 4

HIT. MIDPOINT OF SEGMENT
TRANSDUCER B OUTPUT

A) 7.62 mm BALL AMMO — 2780 ft-lbs

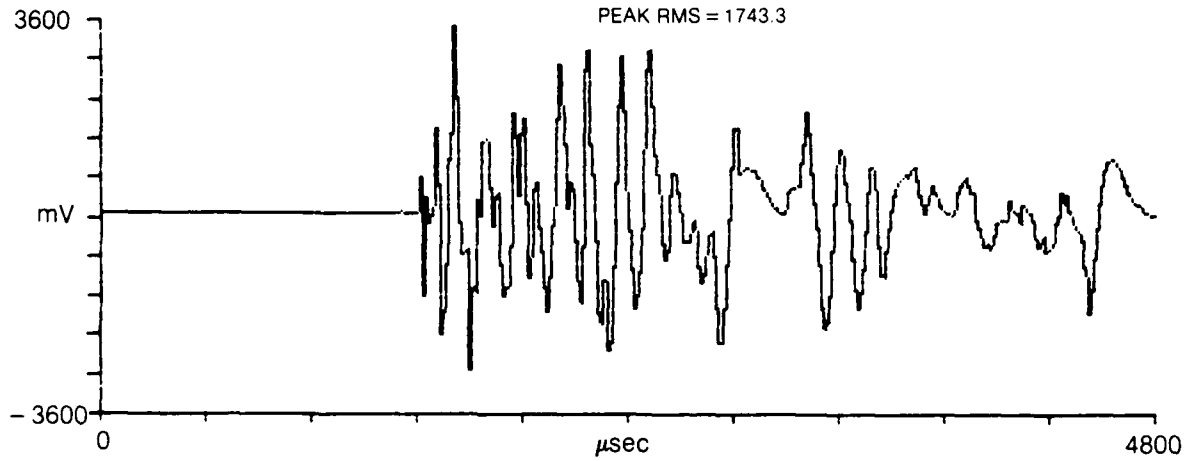

B) 5.6 mm AMMO — 98 ft-lbs

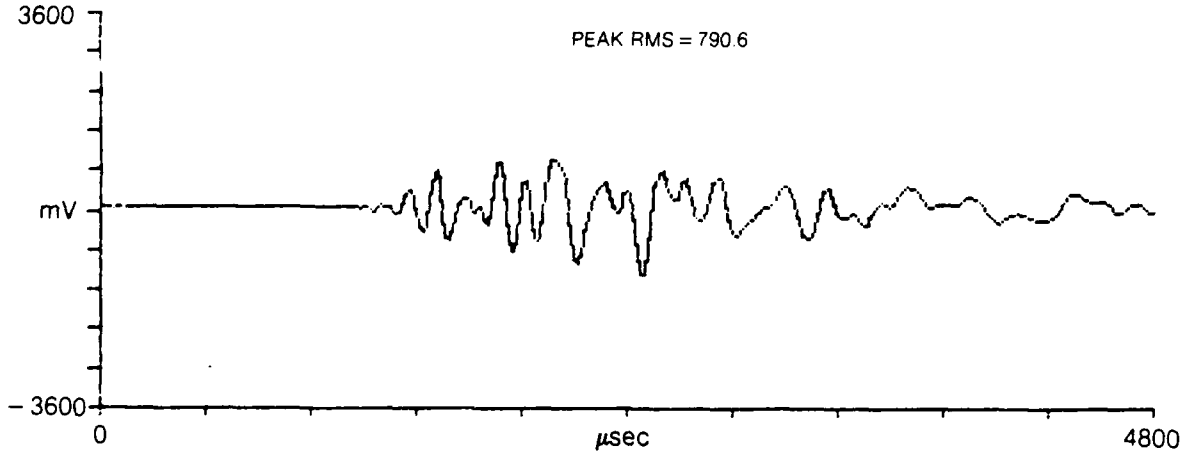

85–11–28–13

FIG. 20

TEST PANEL SEGMENT NO. 5 — FRONT VIEW

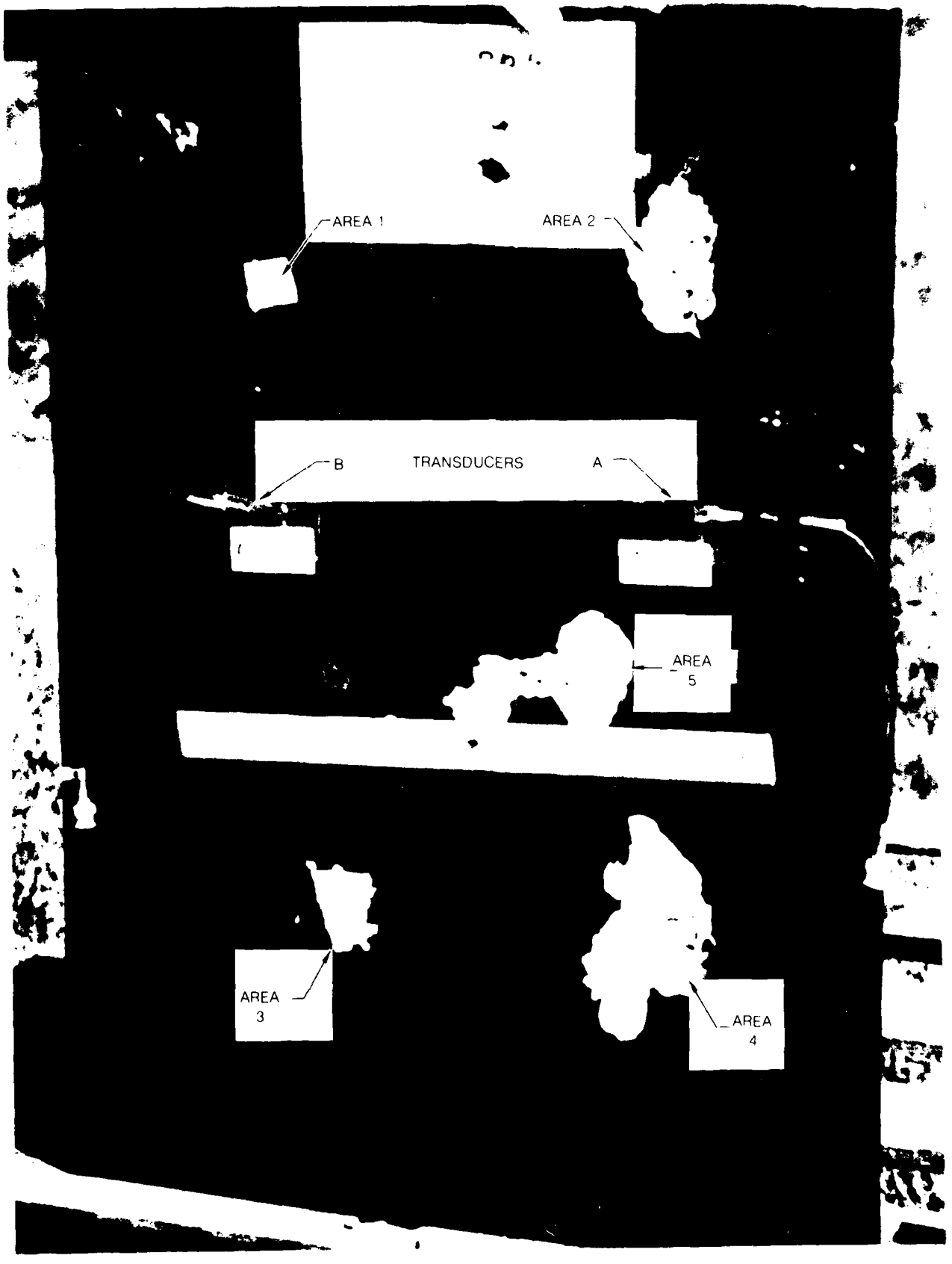

85-11-28-20

TYPICAL WAVEFORMS — SEGMENT NO. 5

HIT: POSITION 2 – ON SPAR
5.6 mm AMMO

A) TRANSDUCER A OUTPUT

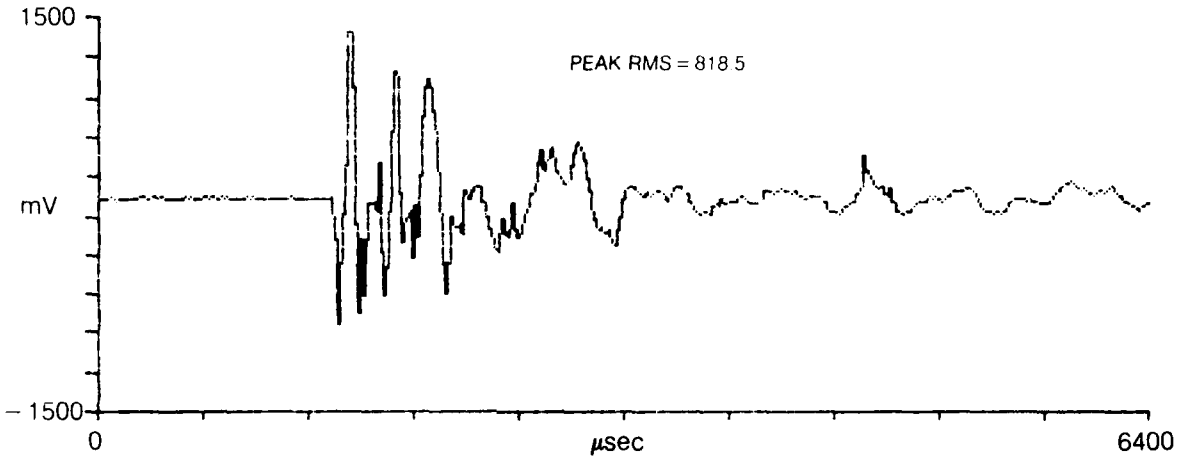

B) TRANSDUCER B OUTPUT

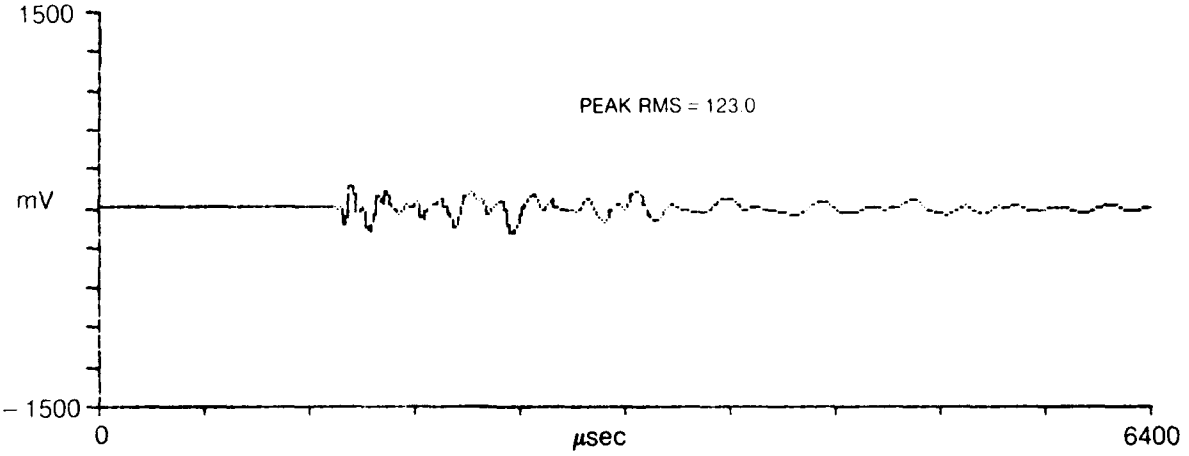

85–11–28–14

TYPICAL WAVEFORMS — SEGMENT NO. 5

HIT. POSITION 1 – OFF SPAR
5.6 mm AMMO

A) TRANSDUCER A OUTPUT

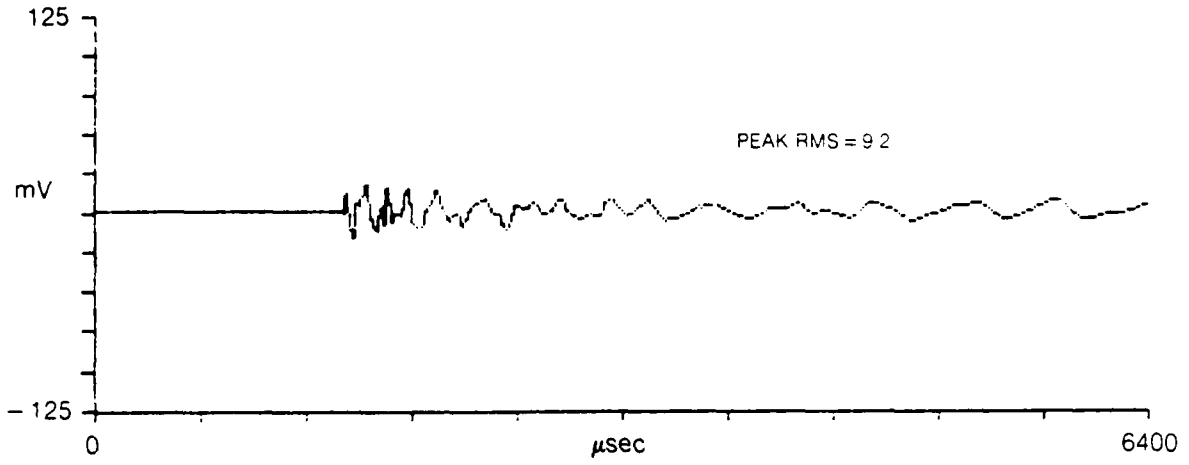

B) TRANSDUCER B OUTPUT

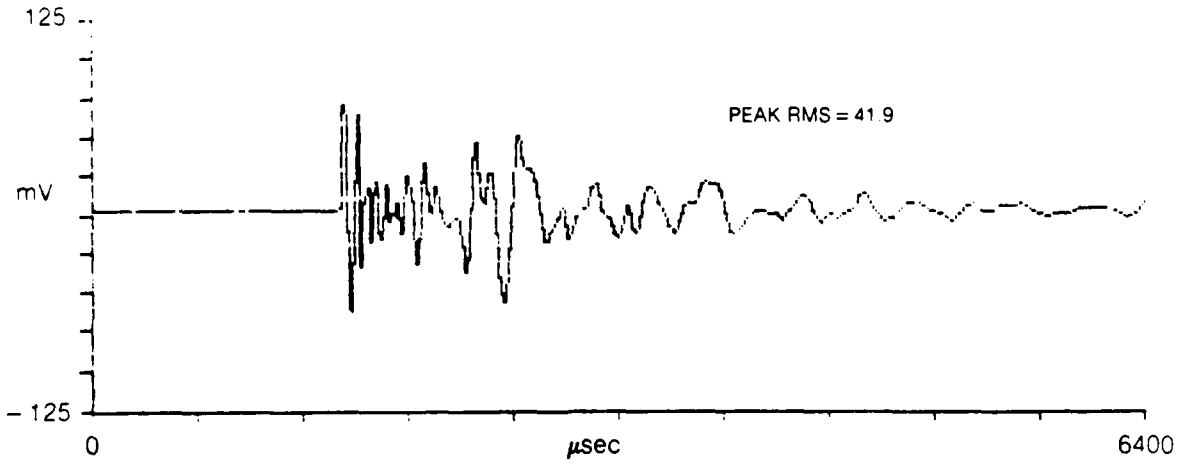

85–11–28–15

TYPICAL AMPLITUDE RMS PLOTS — SEGMENT NO. 5

HIT POSITION 2
5.6 mm AMMO

A) TRANSDUCER A OUTPUT

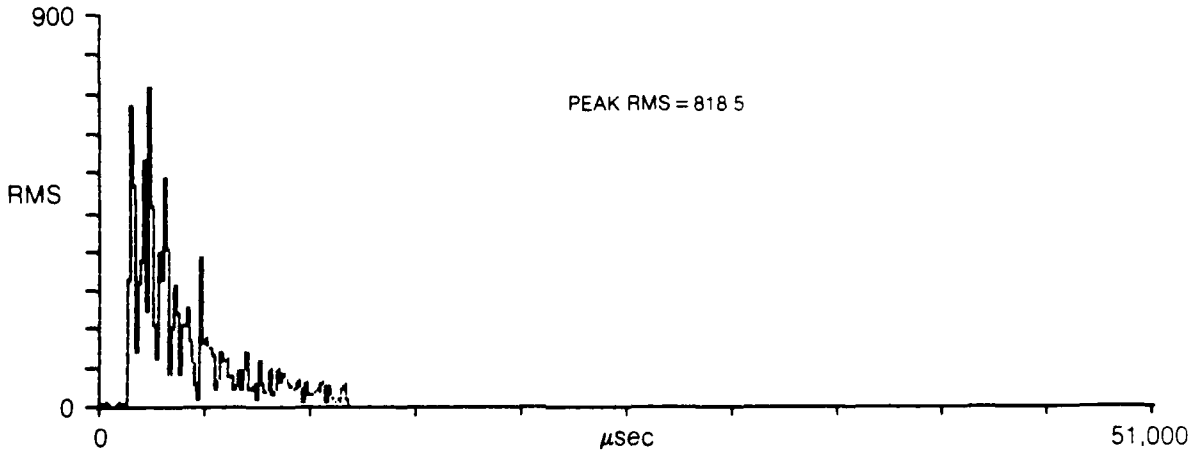

B) TRANSDUCER B OUTPUT

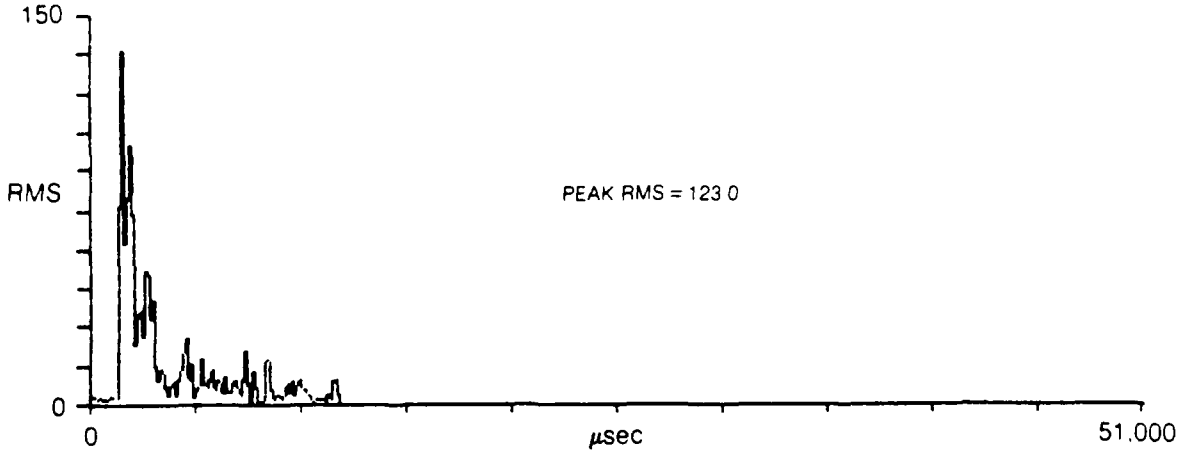

85-11-28-27

PLOT OF COORDINATE SYSTEM FORMED BY EQUAL ARRIVAL TIME DIFFERENCE LOCI

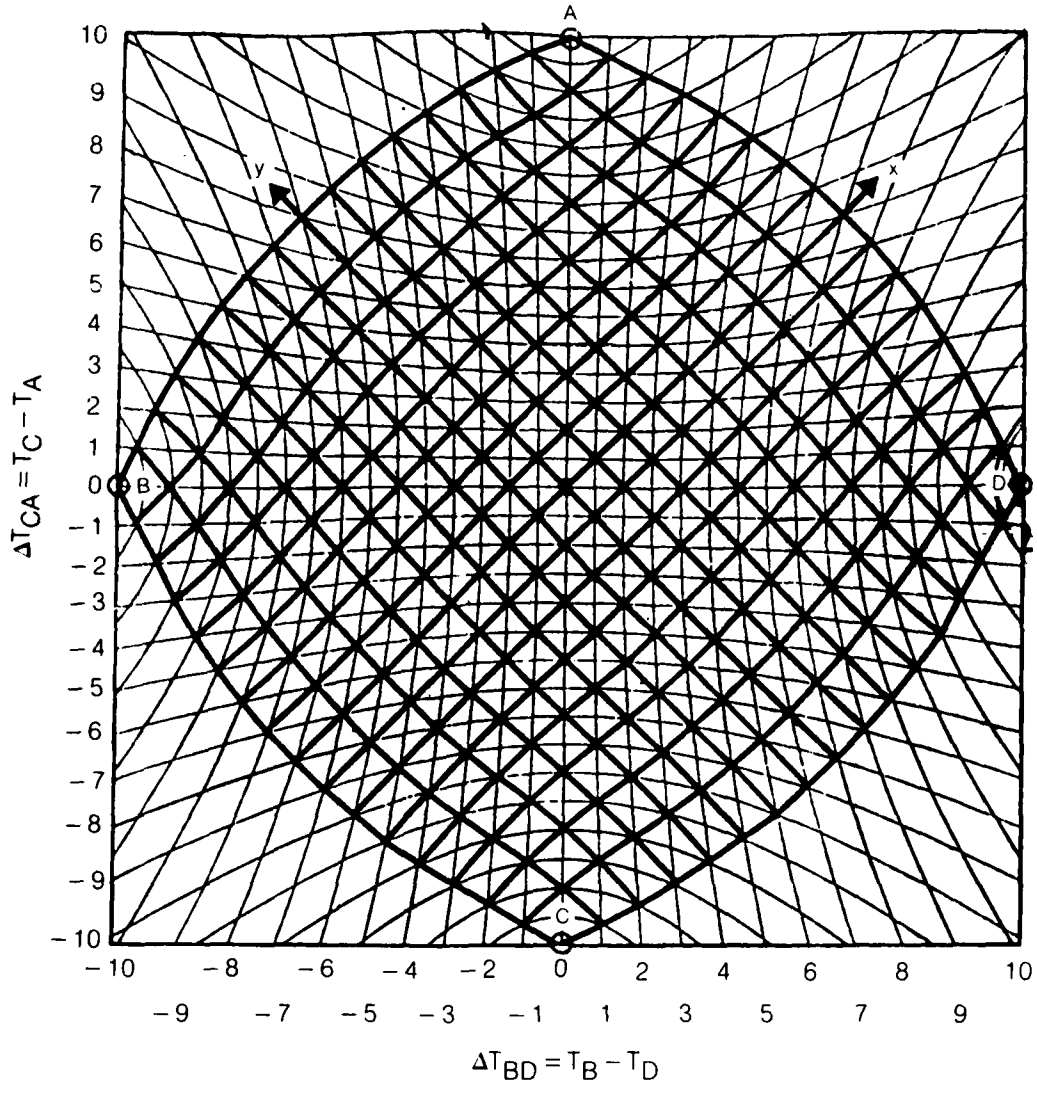

85-11-28-28

FIG. 25

TEST PANEL SEGMENT NO. 6 — FRONT VIEW

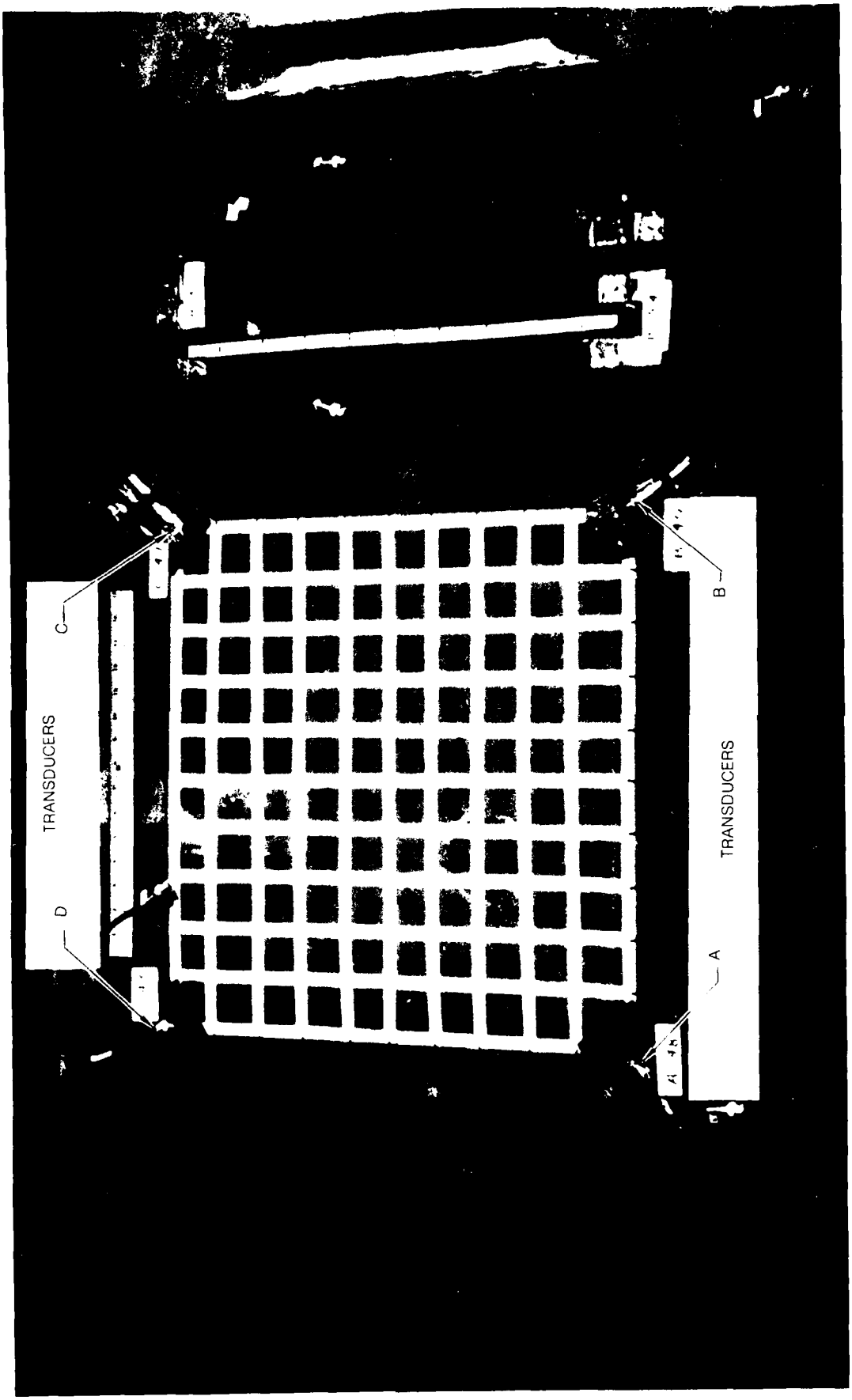

85-11-28-19

FIG. 26

HIT LOCATION RESULTS — SEGMENT NO. 6

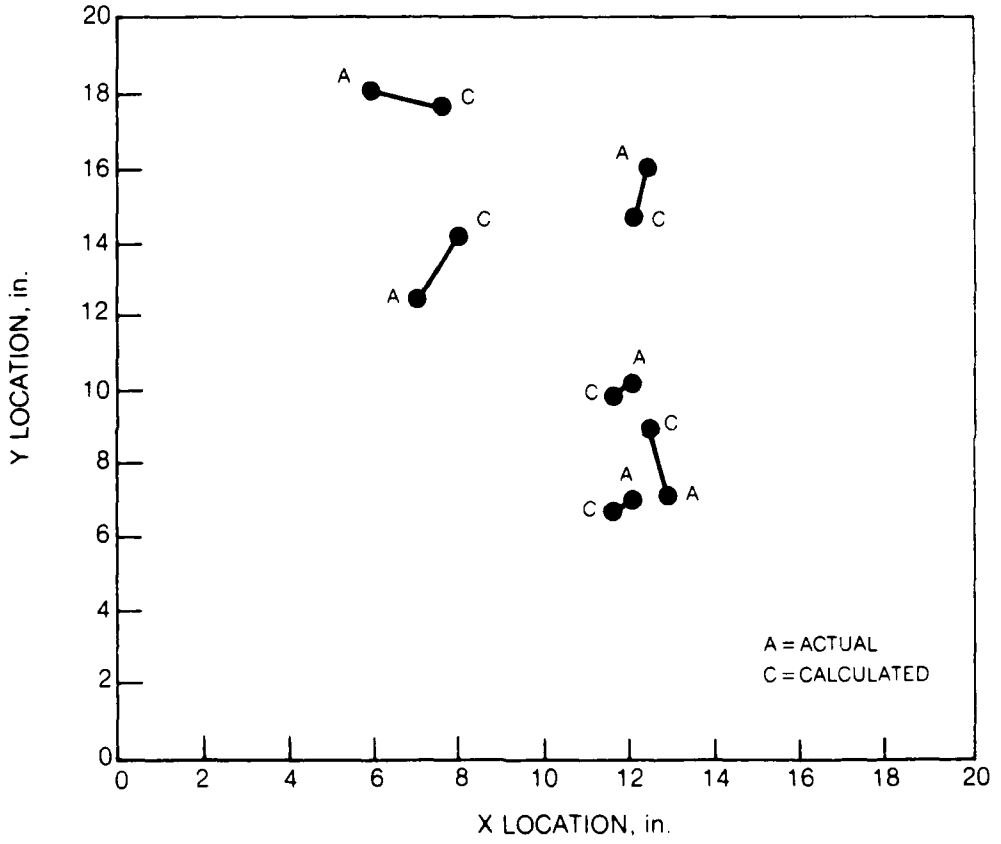

85-11-28-16

SIGNAL ANALYSIS CIRCUITRY

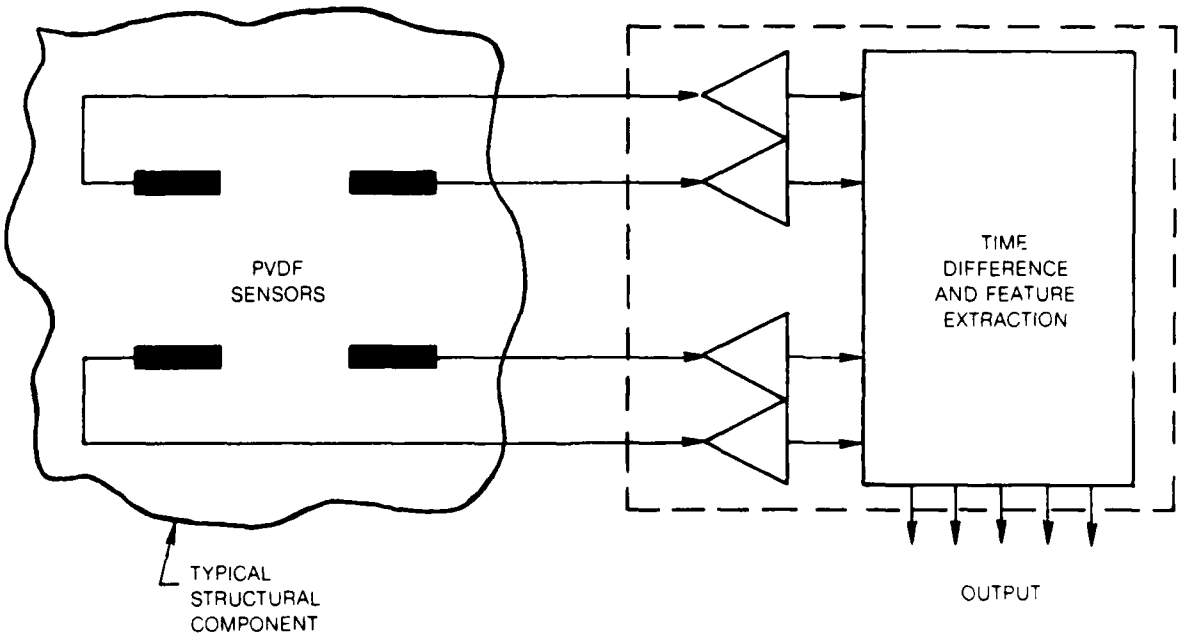

85-11-28-17

FEATURE EXTRACTION CIRCUITRY

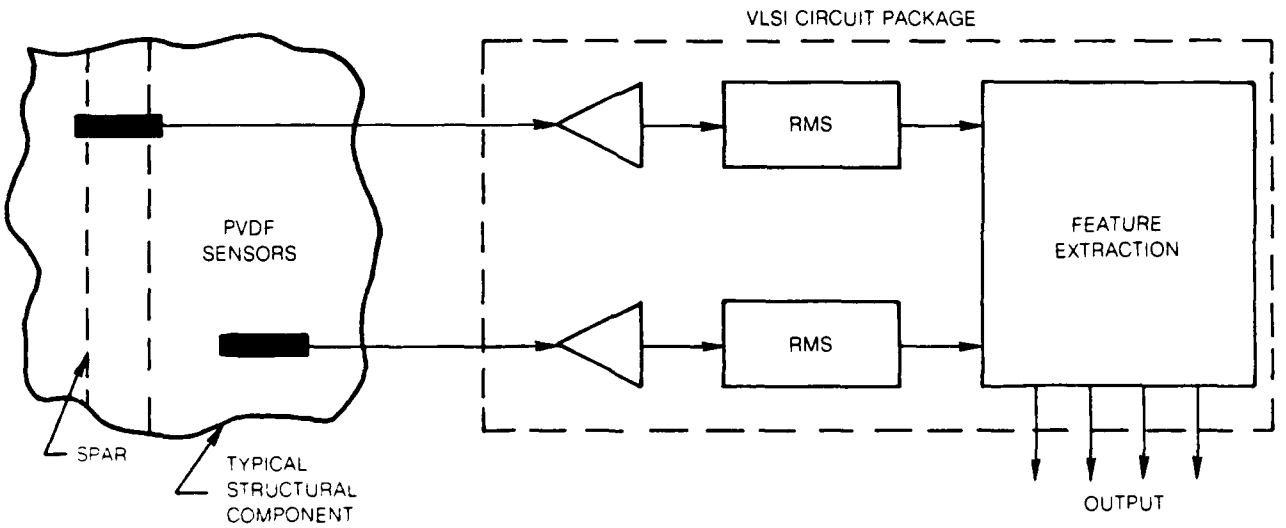

85-11-28-18

APPENDIX - DATA SUMMARY

List of Ballistic Impacts With Resulting Peak RMS Signal Output

Test Panel Segment No. 1

Shot No.	Hit Position (Ref. Fig. 6)	Cartridge	Transducer I.D.	Peak RMS Signal Value
1	4	5.6 mm	A	169.26
			B	225.25
			C	225.24
2	1		A	1052.67
			C	48.42
3			A	782.97
			C	50.11
4	2		A	424.64
			B	36.52
			C	20.63
5			A	324.92
			C	21.19
6			A	246.86
			C	25.76
7			A	242.33
			C	23.42
8	5		A	464.05
			C	280.77
9			A	391.31

APPENDIX - DATA SUMMARY

List of Ballistic Impacts With Resulting Peak RMS Signal Output

Test Panel Segment No. 2

Shot No.	Hit Position (Ref. Figs. 10 & 13)	Cartridge	Transducer I.D.	Peak RMS Signal Value
2*	10*	5.6 mm	C	36.20
			D	32.40
4*			C	40.05
			D	82.03
5*	7*		C	59.06
6*	8*		D	41.77
9*	5*		C	20.43
1	Centered	7.62mm	C	8.57
			D	28.28
2			C	12.34
			D	52.74
3			C	18.32
			D	27.97
4			C	16.10
			D	45.91
5			C	19.46
			D	48.68

*Segment located behind segment No. 3; position nos. marked on segment No. 3

APPENDIX - DATA SUMMARY

List of Ballistic Impacts With Resulting Peak RMS Signal Output

Test Panel Segment No. 3

Shot No.	Hit Position (Ref. Figs. 13 & 14)	Cartridge	Transducer I.D.	Peak RMS Signal Value
2	10	5.6 mm	A	50.35
4	↓	↓	A	33.01
	↓	↓	B	48.94
5	7	↓	B	142.78
6	8	↓	A	37.90
	↓	↓	B	122.37
7	2	↓	A	48.29
	↓	↓	B	58.29
8	↓	↓	A	29.23
	↓	↓	B	35.41
9	5	↓	A	27.83
	↓	↓	B	58.57
14	Off-Spar	6.2 mm	A	22.14
15	On-Spar	↓	A	23.32
16	↓	↓	A	20.63
17	Off-Spar	↓	A	21.16

APPENDIX - DATA SUMMARY

List of Ballistic Impacts With Resulting Peak RMS Signal Output

Test Panel Segment No. 4

Shot No.	Hit Position (Ref. Fig. 17)	Cartridge	Transducer I.D.	Peak RMS Signal Value
4	Near B	7.62 mm	A	1265.88
			B	2168.95
5	Center	7.62 mm APM2	A	1077.40
			B	1501.32
6	Near A	7.62 mm	A	2812.37
			B	1743.33
7	Center		A	1796.14
			B	1898.96
8		7.62 mm Carbine	A	2398.11
			B	1950.86
9			A	2391.66
			B	1494.94
10			A	2506.39
			B	1087.20
11			A	3307.89
			B	1599.65
12	Near A	5.6 mm	B	1139.51
13			B	1033.25
16			A	1155.19
17	Center		A	1942.05
			B	790.60
18			B	1503.40
20	Near B		A	215.66
21			A	121.09
			B	1388.12

APPENDIX - DATA SUMMARY

List of Ballistic Impacts With Resulting Peak RMS Signal Output

Test Panel Segment No. 5

Shot No.	Hit Position (Ref. Fig. 20)	Cartridge	Transducer I.D.	Peak RMS Signal Value
5	3	5.6 mm	A	7.18
			B	24.57
7			B	13.68
8			A	5.48
			B	29.01
9	1		A	39.34
10			A	9.24
			B	41.92
11			A	6.93
			B	30.88
14	4		A	225.46
			B	129.72
15			A	216.74
			B	95.85
16			A	160.22
			B	123.83
17			A	211.26
			B	131.13
18	5		B	96.20
20	2		A	818.50
			B	123.01

APPENDIX - DATA SUMMARY

List of Ballistic Impacts With Resulting
Peak RMS Signal Output

Test Panel Segment No. 5
(Continued)

Shot No.	Hit Position (Ref. Fig. 20)	Cartridge	Transducer I.D.	Peak RMS Signal Value
21	2	5.6 mm	A	791.98
			B	274.37
22			A	657.71
			B	105.99
23			A	257.59
			B	155.68
24	5		A	355.80
			B	277.46
25			A	349.45
			B	271.47
26			A	223.22
			B	370.24
27			B	261.09
29			A	71.96
			B	129.50
31			A	18.74
			B	78.60
33			A	98.64
			B	26.71
34			A	292.46
			B	339.76
35			B	344.38

APPENDIX - DATA SUMMARY

List of Ballistic Impacts With Resulting Time of Arrival

Test Panel Segment No. 6

Shot No.	Hit Position (Ref. Fig. 25)	Cartridge	Transducer I.D.	Time of Arrival μsec
1	5	7.62 mm	A	75.5 *
			B	87.5 *
			C	0.8 *
			D	0 *
2	14		A	98
			B	123
			C	34
			D	0
3	21		A	9.5 *
			B	48.3 *
			C	0 *
			D	29.8 *
4	27		A	89
			B	68
			C	0
			D	38
5	28		A	99.3 *
			B	64.3 *
			C	0 *
			D	46.75*

*Computer generated times; others obtained by hand

APPENDIX - DATA SUMMARY

List of Ballistic Impacts With Resulting Time of Arrival

Test Panel Segment No. 6 (Continued)

Shot No.	Hit Position (Ref. Fig. 25)	Cartridge	Transducer I.D.	Time of Arrival μsec
6	34	7.62 mm	A	44
			B	81
			C	14
			D	0
7	54		A	22
			B	16
			C	0
			D	40
8	64		A	0 *
			B	34.5*
			C	81.0*
			D	39.3*
9	66		A	109.8*
			B	98.5*
			C	0 *
			D	144.0*
10	67		A	21
			B	0
			C	40
			D	65

*Computer generated times; others obtained by hand

APPENDIX - DATA SUMMARY

List of Ballistic Impacts With Resulting Time of Arrival

Test Panel Segment No. 6
(Continued)

Shot No.	Hit Position (Ref. Fig. 25)	Cartridge	Transducer I.D.	Time of Arrival μsec
11	78	7.62 mm	A	0.8*
			B	0 *
			C	13.0*
			D	24.8*
12	79		A	35
			B	0
			C	15
			D	49
13	82		A	0 *
			B	53.0*
			C	42.5*
			D	17.0*

*Computer generated times; others obtained by hand

DISTRIBUTION LIST

No. of Copies	To
1	Office of the Under Secretary of Defense for Research and Engineering, The Pentagon, Washington, DC 20301
2	Commander, Defense Technical Information Center, Cameron Station, Building 5, 5010 Duke Street, Alexandria, VA 22314
1	Metals and Ceramics Information Center, Battelle Columbus Laboratories, 505 King Avenue, Columbus, OH 43201
	Commander, Army Research Office, P.O. Box 12211, Research Triangle Park, NC 27709
1	ATTN: Information Processing Office
	Commander, U.S. Army Materiel Command (AMC), 5001 Eisenhower Avenue, Alexandria, VA 22333
1	ATTN: AMCLD
	Commander, U.S. Army Materiel Systems Analysis Activity, Aberdeen Proving Ground, MD 21005
1	ATTN: AMXSY-MP, H. Cohen
	Commander, U.S. Army Electronics Research and Development Command, Fort Monmouth, NJ 07703
1	ATTN: AMDSD-L
1	AMDSD-E
	Commander, U.S. Army Missile Command, Redstone Arsenal, AL 35898
1	ATTN: AMSMI-RKP, J. Wright, Bldg. 7574
4	AMSMI-TB, Redstone Scientific Information Center
1	AMSMI-RLM
1	Technical Library
	Commander, U.S. Army Armament, Munitions and Chemical Command, Dover, NJ 07801
2	ATTN: Technical Library
1	AMDAR-SCM, J. D. Corrie
1	AMDAR-QAC-E
1	AMDAR-LCA, Mr. Harry E. Pebly, Jr., PLASTEC, Director
	Commander, U.S. Army Natick Research and Development Center, Natick, MA 01760
1	ATTN: Technical Library
	Commander, U.S. Army Satellite Communications Agency, Fort Monmouth, NJ 07703
1	ATTN: Technical Document Center
	Commander, U.S. Army Tank-Automotive Command, Warren, MI 48090
1	ATTN: AMSTA-ZSK
2	AMSTA-UL, Technical Library

No. of Copies	To
	Commander, White Sands Missile Range, NM 88002
1	ATTN: STEWS-WS-VT
	President, Airborne, Electronics and Special Warfare Board, Fort Bragg, NC 28307
1	ATTN: Library
	Director, U.S. Army Ballistic Research Laboratory, Aberdeen Proving Ground, MD 21005
1	ATTN: AMDAR-TSB-S (STINFO)
	Commander, Dugway Proving Ground, Dugway, UT 84022
1	ATTN: Technical Library, Technical Information Division
	Commander, Harry Diamond Laboratories, 2800 Powder Mill Road, Adelphi, MD 20783
1	ATTN: Technical Information Office
	Commander, U.S. Army Laboratory Command, 2800 Powder Mill Road, Adelphi, MD 20783-1197
1	ATTN: Technical Library
	Director, Benet Weapons Laboratory, LCWSL, USA AMCCOM, Watervliet, NY 12189
1	ATTN: AMSMC-LCB-TL
1	AMSMC-LCB-R
1	AMSMC-LCB-RM
1	AMSMC-LCB-RP
	Commander, U.S. Army Foreign Science and Technology Center, 220 7th Street, N.E., Charlottesville, VA 22901
1	ATTN: Military Tech, Mr. Marley
	Commander, U.S. Army Aeromedical Research Unit, P.O. Box 577, Fort Rucker, AL 36360
1	ATTN: Technical Library
	Director, Eustis Directorate, U.S. Army Air Mobility Research and Development Laboratory, Fort Eustis, VA 23604-5577
1	ATTN: Mr. J. Robinson, SAVDL-E-MOS (AVSCOM)
	U.S. Army Aviation Training Library, Fort Rucker, AL 36360
1	ATTN: Building 5906-5907
	Commander, U.S. Army Agency for Aviation Safety, Fort Rucker, AL 36362
1	ATTN: Technical Library
	Commander, USACDC Air Defense Agency, Fort Bliss, TX 79916
1	ATTN: Technical Library
	Commander, U.S. Army Engineer School, Fort Belvoir, VA 22060
1	ATTN: Library

No. of Copies	To
	Commander, U.S. Army Engineer Waterways Experiment Station, P. O. Box 631, Vicksburg, MS 39180
1	ATTN: Research Center Library
	Technical Director, Human Engineering Laboratories, Aberdeen Proving Ground, MD 21005
1	ATTN: Technical Reports Office
	Commandant, U.S. Army Quartermaster School, Fort Lee, VA 23801
1	ATTN: Quartermaster School Library
	Naval Research Laboratory, Washington, DC 20375
1	ATTN: Dr. C. I. Chang - Code 5830
2	Dr. G. R. Yoder - Code 6384
	Chief of Naval Research, Arlington, VA 22217
1	ATTN: Code 471
1	Edward J. Morrissey, AFWAL/MLTE, Wright-Patterson Air Force, Base, OH 45433
	Commander, U.S. Air Force Wright Aeronautical Laboratories, Wright-Patterson Air Force Base, OH 45433
1	ATTN: AFWAL/MLC
1	AFWAL/MLLP, M. Forney Jr.
1	AFWAL/MLBC, Mr. Stanley Schulman
	National Aeronautics and Space Administration, Washington, DC 20546
1	ATTN: Mr. G. C. Deutsch - Code RW
	National Aeronautics and Space Administration, Marshall Space Flight Center, Huntsville, AL 35812
1	ATTN: R. J. Schwinghammer, EH01, Dir, M&P Lab
1	Mr. W. A. Wilson, EH41, Bldg. 4612
	Naval Air Systems Command, Washington, DC 20361-6001
1	ATTN: Dale B. Atkinson, AIR-5164
1	Robert D. Hume, AIR-5262
1	LTCOL James Sebolka, AIR-5164J
1	MAJ Ralph E. Kanko, AIR-5164J2
1	David St. Jean, AIR-53031
	Naval Weapons Center, China Lake, CA 93555-6001
1	ATTN: James J. Childress, Code 3383
1	Conrad Driussi, Code 3382
1	Dr. Eric Lundstrom, Code 3835
1	John J. Morrow, Code 338

No. of Copies	To
	Commander, U.S. Air Force Wright Aeronautical Laboratories, Flight Dynamics Laboratory, FI, Wright-Patterson Air Force Base, OH 45433-6553
1	ATTN: AFWAL/FIESD, L. E. Gilbert
1	AFWAL/FIES, James Hodges
1	AFWAL/FIBC, Larry G. Kelly
1	AFWAL/FIBCA, Cecil D. Wallace
1	Committee on Marine Structures, Marine Board, National Research Council, 2101 Constitution Ave., N. W., Washington, DC 20418
1	Librarian, Materials Sciences Corporation, Guynedd Plaza 11, Bethlehem Pike, Spring House, PA 19477
1	The Charles Stark Draper Laboratory, 68 Albany Street, Cambridge, MA 02139
	Wyman-Gordon Company, Worcester, MA 01601
1	ATTN: Technical Library
	Lockheed-Georgia Company, 86 South Cobb Drive, Marietta, GA 30063
1	ATTN: Materials and Processes Engineering Dept. 71-11, Zone 54
	General Dynamics, Convair Aerospace Division, P.O. Box 748, Fort Worth, TX 76101
1	ATTN: Mfg. Engineering Technical Library
1	Mechanical Properties Data Center, Belfour Stulen Inc., 13917 W. Bay Shore Drive, Traverse City, MI 49684
1	Mr. R. J. Zentner, EAI Corporation, 198 Thomas Johnson Drive, Suite 16, Frederick, MD 21701
	Naval Postgraduate School, Monterey, CA 93943
1	ATTN: Prof. Robert E. Ball, Code 67BP
	NASA Ames Research Center, Chemical Research Projects Office, Moffett Field, CA 94035
1	ATTN: Richard H. Fish, Code SC, M/S N-223-6
	Booz, Allen, and Hamilton Incorporation, 2309 Renard Place SE, Suite 301, Albuquerque, NM 87106
1	ATTN: William J. Herman, Senior Associate
	Naval Air Development Center, Warminster, PA 18974
1	ATTN: Thomas E. Hess, Code 6043
	U.S. Army Research & Technology Laboratories (AVSCOM), Applied Technology Laboratory, Fort Eustis, VA 23604-5577
1	ATTN: Charles M. Pedriani, SAVDL-ATL-ASV

No. of Copies	To
	Naval Research Laboratory, 4555 Overlook Avenue, SW, Washington, DC 20375-5000
1	ATTN: Dr. Fred R. Stonesifer, Code 5832
	U.S. Army Ballistic Research Lab, ARDC, AMCCOM, Aberdeen Proving Ground, MD 21005-5066
1	ATTN: Walter S. Vikestad, AMXBR-BLV-A
	Director, Department of Energetic Systems, Southwest Research Institute, P.O. Drawer 28510, 6220 Culebera Road, San Antonio, TX 78284
1	ATTN: Alex B. Wenzel
	Director, U.S. Army Materials Technology Laboratory, Watertown, MA 02172-0001
2	ATTN: SLCMT-IML
10	SLCMT-MSR, R. Muldoon
1	SLCMT-IMA-P
1	SLCMT-ISC

Army Materials Technology Laboratory

AD ______________

Watertown, Massachusetts 02172-0001
FINAL REPORT: DETECTION AND LOCATION OF BALLISTIC DAMAGE IN COMPOSITE MATERIALS USING ACOUSTIC EMISSION METHODS
Jeorme F. Jaminet, Michael W. Havman and Richard S. Williams
United Technologies Research Center
East Hartford, CT 06108
Technical Report MTL TR85-37, December 1985, 62 pp. illus - tables, Contract DAAG46-84-C-0054
Final Report, Sept. 1984 to Oct. 1985

UNCLASSIFIED
UNLIMITED DISTRIBUTION

Key Words

Ballistic hits
Battle damage
Composites
Helicopter
Survivability

A method for increasing survivability is described whereby the acoustic emissions generated by ballistic impacts on composite helicopter structural components are recorded and analyzed using a preliminary digital transient data recording test system, the Digital Acoustic Emission System (DAES) and lightweight sensors utilizing polyvinylidene fluoride (PVDF) film. A total of 77 ballistic impacts on six composite test segments using a variety of fragment simulating projectiles (FSP) with different muzzle velocities and impact energies is described. The results verify the capability of the measurement system to detect, locate, and analyze the severity of the ballistic impacts. The ratio of the peak RMS value of the output signal from two sensors is shown to be a good indicator of impact energy absorption or damage severity. Calculated hit locations are found with a mean error of seven percent of the sensor array edge distance.

Army Materials Technology Laboratory

AD ______________

Watertown, Massachusetts 02172-0001
FINAL REPORT: DETECTION AND LOCATION OF BALLISTIC DAMAGE IN COMPOSITE MATERIALS USING ACOUSTIC EMISSION METHODS
Jeorme F. Jaminet, Michael W. Havman and Richard S. Williams
United Technologies Research Center
East Hartford, CT 06108
Technical Report MTL TR85-37, December 1985, 62 pp. illus - tables, Contract DAAG46-84-C-0054
Final Report, Sept. 1984 to Oct. 1985

UNCLASSIFIED
UNLIMITED DISTRIBUTION

Key Words

Ballistic hits
Battle damage
Composites
Helicopter
Survivability

A method for increasing survivability is described whereby the acoustic emissions generated by ballistic impacts on composite helicopter structural components are recorded and analyzed using a preliminary digital transient data recording test system, the Digital Acoustic Emission System (DAES) and lightweight sensors utilizing polyvinylidene fluoride (PVDF) film. A total of 77 ballistic impacts on six composite test segments using a variety of fragment simulating projectiles (FSP) with different muzzle velocities and impact energies is described. The results verify the capability of the measurement system to detect, locate, and analyze the severity of the ballistic impacts. The ratio of the peak RMS value of the output signal from two sensors is shown to be a good indicator of impact energy absorption or damage severity. Calculated hit locations are found with a mean error of seven percent of the sensor array edge distance.

Army Materials Technology Laboratory

AD ______________

Watertown, Massachusetts 02172-0001
FINAL REPORT: DETECTION AND LOCATION OF BALLISTIC DAMAGE IN COMPOSITE MATERIALS USING ACOUSTIC EMISSION METHODS
Jeorme F. Jaminet, Michael W. Havman and Richard S. Williams
United Technologies Research Center
East Hartford, CT 06108
Technical Report MTL TR85-37, December 1985, 62 pp. illus - tables, Contract DAAG46-84-C-0054
Final Report, Sept. 1984 to Oct. 1985

UNCLASSIFIED
UNLIMITED DISTRIBUTION

Key Words

Ballistic hits
Battle damage
Composites
Helicopter
Survivability

A method for increasing survivability is described whereby the acoustic emissions generated by ballistic impacts on composite helicopter structural components are recorded and analyzed using a preliminary digital transient data recording test system, the Digital Acoustic Emission System (DAES) and lightweight sensors utilizing polyvinylidene fluoride (PVDF) film. A total of 77 ballistic impacts on six composite test segments using a variety of fragment simulating projectiles (FSP) with different muzzle velocities and impact energies is described. The results verify the capability of the measurement system to detect, locate, and analyze the severity of the ballistic impacts. The ratio of the peak RMS value of the output signal from two sensors is shown to be a good indicator of impact energy absorption or damage severity. Calculated hit locations are found with a mean error of seven percent of the sensor array edge distance.

Army Materials Technology Laboratory

AD ______________

Watertown, Massachusetts 02172-0001
FINAL REPORT: DETECTION AND LOCATION OF BALLISTIC DAMAGE IN COMPOSITE MATERIALS USING ACOUSTIC EMISSION METHODS
Jeorme F. Jaminet, Michael W. Havman and Richard S. Williams
United Technologies Research Center
East Hartford, CT 06108
Technical Report MTL TR85-37, December 1985, 62 pp. illus - tables, Contract DAAG46-84-C-0054
Final Report, Sept. 1984 to Oct. 1985

UNCLASSIFIED
UNLIMITED DISTRIBUTION

Key Words

Ballistic hits
Battle damage
Composites
Helicopter
Survivability

A method for increasing survivability is described whereby the acoustic emissions generated by ballistic impacts on composite helicopter structural components are recorded and analyzed using a preliminary digital transient data recording test system, the Digital Acoustic Emission System (DAES) and lightweight sensors utilizing polyvinylidene fluoride (PVDF) film. A total of 77 ballistic impacts on six composite test segments using a variety of fragment simulating projectiles (FSP) with different muzzle velocities and impact energies is described. The results verify the capability of the measurement system to detect, locate, and analyze the severity of the ballistic impacts. The ratio of the peak RMS value of the output signal from two sensors is shown to be a good indicator of impact energy absorption or damage severity. Calculated hit locations are found with a mean error of seven percent of the sensor array edge distance.

Army Materials Technology Laboratory
Watertown, Massachusetts 02172-0001
FINAL REPORT: DETECTION AND LOCATION OF BALLISTIC DAMAGE IN COMPOSITE MATERIALS USING ACOUSTIC EMISSION METHODS
Jeorme P. Jaminet, Michael V. Havman and Richard S. Williams
United Technologies Research Center
East Hartford, CT 06108
Technical Report MTL TR85-37, December 1985, 62 pp. illus - tables, Contract DAAG46-84-C-0054
Final Report, Sept. 1984 to Oct. 1985

AD ____________

UNCLASSIFIED
UNLIMITED DISTRIBUTION

Key Words

Ballistic hits
Battle damage
Composites
Helicopter
Survivability

A method for increasing survivability is described whereby the acoustic emissions generated by ballistic impacts on composite helicopter structural components are recorded and analyzed using a preliminary digital transient data recording test system, the Digital Acoustic Emission System (DAES) and lightweight sensors utilizing polyvinylidene fluoride (PVDF) film. A total of 77 ballistic impacts on six composite test segments using a variety of fragment simulating projectiles (FSP) with different muzzle velocities and impact energies is described. The results verify the capability of the measurement system to detect, locate, and analyze the severity of the ballistic impacts. The ratio of the peak RMS value of the output signal from two sensors is shown to be a good indicator of impact energy absorption or damage severity. Calculated hit locations are found with a mean error of seven percent of the sensor array edge distance.

Army Materials Technology Laboratory
Watertown, Massachusetts 02172-0001
FINAL REPORT: DETECTION AND LOCATION OF BALLISTIC DAMAGE IN COMPOSITE MATERIALS USING ACOUSTIC EMISSION METHODS
Jeorme P. Jaminet, Michael V. Havman and Richard S. Williams
United Technologies Research Center
East Hartford, CT 06108
Technical Report MTL TR85-37, December 1985, 62 pp. illus - tables, Contract DAAG46-84-C-0054
Final Report, Sept. 1984 to Oct. 1985

AD ____________

UNCLASSIFIED
UNLIMITED DISTRIBUTION

Key Words

Ballistic hits
Battle damage
Composites
Helicopter
Survivability

A method for increasing survivability is described whereby the acoustic emissions generated by ballistic impacts on composite helicopter structural components are recorded and analyzed using a preliminary digital transient data recording test system, the Digital Acoustic Emission System (DAES) and lightweight sensors utilizing polyvinylidene fluoride (PVDF) film. A total of 77 ballistic impacts on six composite test segments using a variety of fragment simulating projectiles (FSP) with different muzzle velocities and impact energies is described. The results verify the capability of the measurement system to detect, locate, and analyze the severity of the ballistic impacts. The ratio of the peak RMS value of the output signal from two sensors is shown to be a good indicator of impact energy absorption or damage severity. Calculated hit locations are found with a mean error of seven percent of the sensor array edge distance.

Army Materials Technology Laboratory
Watertown, Massachusetts 02172-0001
FINAL REPORT: DETECTION AND LOCATION OF BALLISTIC DAMAGE IN COMPOSITE MATERIALS USING ACOUSTIC EMISSION METHODS
Jeorme P. Jaminet, Michael V. Havman and Richard S. Williams
United Technologies Research Center
East Hartford, CT 06108
Technical Report MTL TR85-37, December 1985, 62 pp. illus - tables, Contract DAAG46-84-C-0054
Final Report, Sept. 1984 to Oct. 1985

AD ____________

UNCLASSIFIED
UNLIMITED DISTRIBUTION

Key Words

Ballistic hits
Battle damage
Composites
Helicopter
Survivability

A method for increasing survivability is described whereby the acoustic emissions generated by ballistic impacts on composite helicopter structural components are recorded and analyzed using a preliminary digital transient data recording test system, the Digital Acoustic Emission System (DAES) and lightweight sensors utilizing polyvinylidene fluoride (PVDF) film. A total of 77 ballistic impacts on six composite test segments using a variety of fragment simulating projectiles (FSP) with different muzzle velocities and impact energies is described. The results verify the capability of the measurement system to detect, locate, and analyze the severity of the ballistic impacts. The ratio of the peak RMS value of the output signal from two sensors is shown to be a good indicator of impact energy absorption or damage severity. Calculated hit locations are found with a mean error of seven percent of the sensor array edge distance.

Army Materials Technology Laboratory
Watertown, Massachusetts 02172-0001
FINAL REPORT: DETECTION AND LOCATION OF BALLISTIC DAMAGE IN COMPOSITE MATERIALS USING ACOUSTIC EMISSION METHODS
Jeorme P. Jaminet, Michael V. Havman and Richard S. Williams
United Technologies Research Center
East Hartford, CT 06108
Technical Report MTL TR85-37, December 1985, 62 pp. illus - tables, Contract DAAG46-84-C-0054
Final Report, Sept. 1984 to Oct. 1985

AD ____________

UNCLASSIFIED
UNLIMITED DISTRIBUTION

Key Words

Ballistic hits
Battle damage
Composites
Helicopter
Survivability

A method for increasing survivability is described whereby the acoustic emissions generated by ballistic impacts on composite helicopter structural components are recorded and analyzed using a preliminary digital transient data recording test system, the Digital Acoustic Emission System (DAES) and lightweight sensors utilizing polyvinylidene fluoride (PVDF) film. A total of 77 ballistic impacts on six composite test segments using a variety of fragment simulating projectiles (FSP) with different muzzle velocities and impact energies is described. The results verify the capability of the measurement system to detect, locate, and analyze the severity of the ballistic impacts. The ratio of the peak RMS value of the output signal from two sensors is shown to be a good indicator of impact energy absorption or damage severity. Calculated hit locations are found with a mean error of seven percent of the sensor array edge distance.